POLITECNICO DI TORINO

Master Degree in Biomedical Engineering

Molecular modelling to investigate tubulin conformational dynamics driven by antimitotic agents

Thesis Supervisor
Prof. Marco Agostino Deriu

Candidate
Valentina Ripa

ACADEMIC YEAR 2019-2020

Contents

ABSTRACT

Microtubules (MT) play key roles in cell mitosis and in particular they help to segregate chromosomes. For this reason, MTs are a desirable target in cancer treatment for the inhibition of the unregulated tumoral cells division. In addition, several tubulin isotypes exist, each one having its own sensitivity to a specific drug and a different level of expression depending on tissues. This represents an important opportunity in drug design, which may exploit tubulin isotypes expression to study and synthesize highly specific drugs, having a greater affinity only for diseased cells and causing reduced systemic effects. Antimitotic drugs act by interfering with MT polymerization-depolymerization kinetics, but the molecular mechanisms responsible for the drug activity is still unclear. These drugs can be classified according to their effects on MT dynamics. In this work, we have considered one stabilizing agent, i.e. Taxol, and a destabilizing one, i.e. Colchicine. More in detail, molecular modelling has been employed to investigate the effects of these drugs on the conformational behaviour expressed by two different human tubulin isotypes. Results of the present research might shed light on the molecular mechanism of action of investigated drugs and thus make clearer the induced tubulin conformational modifications which affect the entire MT dynamics.

1 Introduction

This chapter provides a general introduction to this Master's Thesis work, summarising the biological background, the research objectives and organization of the presented work.

Microtubules (MT) are cytoskeleton filaments playing crucial roles in eukaryotic cells, such as cell shape maintenance, cell signalling and mitosis. More in detail they constitute the mitotic spindle with the purpose of dividing the chromosomes between the two daughter cells. MTs are composed by α and β tubulin heterodimers organised into linear protofilaments, which interact laterally with each other, creating a hollow cylindrical polymer. MTs are characterized by a dynamic equilibrium between states of rapid growing and fast disassembly: this behaviour is commonly identified as *dynamic instability* and it is essential for the proper execution of all tasks. The polymerization process is still unclear but what is certain is that it is influenced by the conformational state of the dimer. Dynamic equilibrium alteration can have important consequences on the cell cycle, and possibly lead to the arrest of mitosis and cell death. The alteration of dynamic instability caused using antimitotic drugs, like Colchicine and Taxol, is particularly exploited in anti-cancerous therapies. Different tubulin isotypes are expressed in human tissues, and the same compound binds them with different affinity. Moreover, the expression of isotypes also changes according to external stimuli suffered by the cell, such as exposure to anticancer drugs: this represents an opportunity to rationally refine the compound design, by searching for ligands with greater effectiveness and capable of causing fewer systemic effects.
In recent years, the use of computational techniques has increased significantly, especially thanks to the improvements introduced in the field of computer science. More in detail, nowadays it is possible to simulate biological systems consisting of a huge number of molecules. These biological systems and their physical properties can be studied with atomistic resolution thanks to different tools, such as Molecular Dynamics (MD).

The aim of the present research study is to deepen the knowledge on the mechanisms of action of two well known drugs, Colchicine and Taxol. More in detail this study investigates the molecular phenomena characterizing their binding the two most expressed human tubulin isotypes. With this purpose, molecular dynamics simulations (MD) have been employed focusing attention both on the local effects introduced by the presence of the drug and on the tubulin dimer conformational changes, which drive the dynamics of the microtubule.

The Master's Thesis here presented is divided into the following chapters.

Chapter 1 is the present introduction.

Chapter 2 contains a description of the methods employed in this work. The physical and theoretical aspects of Molecular Mechanics and Molecular Dynamics are described.

Chapter 3 introduces the biological background of the MT: tubulin structure, polymerization process, microtubule instability, isotypes expression and MT targeting agents are described.

Chapter 4 is dedicated to the main original work of this Master's Thesis. Conformational changes induced on tubulin dimer due to interaction with two drugs, Colchicine and Taxol, have been investigated by molecular modelling. Two different tubulin isotypes, I and IVb, have been considered in this study. Among all the molecular phenomena induced by compound binding, both local effects near the binding site and global effects, such as bending and twisting angles, have been investigated.

2 Material and methods

The following chapter provides a description of theoretical and physical bases underlying the computational methods used in the development of this Master Thesis. In particular, Molecular Modelling, Molecular Mechanics and Molecular Dynamics are described.

2.1 Molecular modelling

Molecular modelling comprises all theoretical and computational techniques used to study and describe behaviour and properties of chemical systems, from simpler ones to complex ones, like proteins, polymers, molecules, nucleic acids.

The most rigorous way to describe a molecular system is to observe it at the Quantum Mechanical (QM) level, solving approximations of the Schrödinger's equation. However, the so called ab-initio methods are only applicable for very small systems, at most composed by a few hundreds of atoms.
Nevertheless, phenomena related to biological systems require larger and more complex systems than those described through ab-initio methodologies. Therefore, a classical approach such as Molecular Mechanics (MM) is generally employed, since it allows to describe and study larger systems made of hundred thousands of atoms. The MM does not consider electron's motion in the system description but it employs a potential energy function called force-field, which keeps into account only for atomic nuclear position. This is the starting point to describe the molecular or macromolecular system. Then, sampling methodology like Monte Carlo approach or Molecular Dynamics can be used on MM models to predict macroscopic properties of biological systems, and investigate molecular processes such as protein conformational behaviour, ligand binding, and so on (Leach 2001).

2.2 Molecular Mechanics

In Molecular Mechanics, atoms are approximated in spheres having an own radius and an own charge connected by bonds modelled by springs, characterized by a certain stiffness value. Radius, charge and stiffness values are determined from both theory and experimental measurements. Through the *force field* (FF, a set of equations), it is possible to calculate the *potential energy V* as a function of only atoms positions. Using this set of equations, it is possible to solve Newton's equations of motion.

2.2.1 Potential Energy Function

One of the aims of MD simulations is to explore the phase space and define the energy value associated to each configuration. The potential energy function describes the portion of the total energy of the system not due to the atoms motion and it has two contribution, one relating to covalent bonds among atom pairs and one relating to non-covalent interaction (electrostatic and Van Der Waals).

$$V = V_{bonded} + V_{non-bonded} \tag{1}$$

Bonded and non-bonded contributions can be defined as follows:

$$V_{bonded} = V_{bond} + V_{angle} + V_{dihedral} \tag{2}$$

$$V_{non-bonded} = V_{VdW} + V_{Coulomb} \tag{3}$$

Each one of the terms here reported can be implemented in different ways, depending on the chosen FF in simulation settings.

2.2.2 Bonded and non-bonded interactions

The potential energy function can be written as:

$$V(r_N) = \sum_{Bonds} \frac{1}{2} k_l [l - l_0]^2 + \sum_{Angles} \frac{1}{2} k_\vartheta [\vartheta - \vartheta_0]^2 + \sum_{Dihedrals} k_\varphi [1 + \cos\ (n\varphi + \delta)] + \\ + \sum_{i=1}^{N} \sum_{j=i+1}^{N} 4\varepsilon_{i,j} \left[\left(\frac{\sigma_{i,j}}{r_{i,j}} \right)^{12} - \left(\frac{\sigma_{i,j}}{r_{i,j}} \right)^{6} \right] + \frac{Q_j Q_i}{4\pi\varepsilon_0 \varepsilon_r r_{i,j}} \tag{4}$$

The first three summaries relate to terms depending on internal coordinates, that is bond lengths, bond angles and dihedrals.

Bond lengths term is modelled with harmonic potential:

$$V_{bond} = \sum_{Bonds} \frac{1}{2} k_l [l - l_0]^2 \tag{5}$$

Potential energy particularly rises when bond length increases or decreases with respect to the reference value l_0, the equilibrium length. k_l is the bond stiffness. Both l_0 and k_l are defined for each atom pair and their values depends on the atom types.

Bond angles are defined by three atoms, and their energy term is modelled with harmonic potential too:

$$V_{angles} = \sum_{Angles} \frac{1}{2} k_\vartheta [\vartheta - \vartheta_0]^2 \quad (6)$$

ε_{ijk} is the equilibrium angle and k_ϑ is the angle stiffness.

Rotation is defined by taking into account four atoms and the dihedral angle, the angle formed between the plane identified by the first three atoms and the plane identified by the last three atoms.

$$V_{dihedral} = \sum_{Dihedrals} k_\varphi [1 + \cos\ (n\varphi - \varphi_0)] \quad (7)$$

ϕ is the dihedral angle between planes, ϕ_0 is the dihedral angel at the equilibrium and k_ϕ is the dihedral stiffness.

The last term describes interactions among not covalently bound atom. It is made up of two contributions, the long-range or Coulomb interactions and short-range or Van del Waals interactions. Compared to bonded ones, those interactions are very weak, but they are equally important in defining the system and its properties correctly.
Coulomb interactions energies are modelled as follows:

$$V_{Coulomb} = \frac{Q_j Q_i}{4\pi\varepsilon_0 \varepsilon_r r_{i,j}} \quad (8)$$

Q_i and Q_j are the two atom charges, ε_0 is the vacuum permittivity, ε_r is the relative permittivity and r_{ij} is the distance between two atoms.
Van der Waals energies are described through the Lennard-Jones 12-6 equation, which models the interaction between a pair of neutral atoms:

$$V_{VdW} = 4\varepsilon_{i,j}\left[\left(\frac{\sigma_{i,j}}{r_{i,j}}\right)^{12} - \left(\frac{\sigma_{i,j}}{r_{i,j}}\right)^{6}\right] \quad (9)$$

The term with 12 as exponent describes the repulsion among two atoms because of overlapping of the electron orbitals, while the term with 6 as exponent describes the attraction among the two. r_{ij} is the distance between the two atoms involved, σ_{ij} is the collision diameter, namely the distance at which the Van der Waals potential is null and ε_{ij} is the minimum reached by Van del Waals potential function. Van der Waals interactions are referred to as short range interactions because their value goes down faster than Coulomb interactions, being the terms to the denominator raised to the power of 12 or 6 unlike terms in Coulomb law.

The most computationally expensive interactions are the non-bonded ones, as they grow with the square of the number of atoms. Their calculation can be simplified by adopting adequate methods, like the *distance cutoff*, allowing for calculating non-bonded interaction only for atom pairs with distance smaller than cutoff. Anyway, it could generate artefact in long range interactions. That's why other methods had been introduced, like shift and switched cut-off, that avoid suddenly cancelling interactions beyond the cutoff, or Ewald summation, which sums interaction energies in Fourier space rather than in real space, a method widely employed in long-range interactions calculation (Hark Lee and Cai 2009; Darden, York, and Pedersen 1993; Hsing Lee et al. 2002).

2.2.3 Periodic boundary Conditions

In order to proceed with simulations, the atomic system is placed in a box usually filled with implicit or explicit water model or other solvents. Boxes may vary in shape and size, but all of them cause imprecisions because of the artificial unrealistic boundary introduced with the vacuum. In order to correct this behaviour, the *periodic boundary conditions (PBCs)* are applied, which still cause inaccuracies but less severe. This method consists in surrounding the analysed box by copies of itself (Figure 2.1), allowing near boundary particles to interact with other particles located outside the box and placed in the copied one. In this case dimensions must be settled so as to avoid a particle to interact with itself, thus respecting the so-called *minimum image convention*.

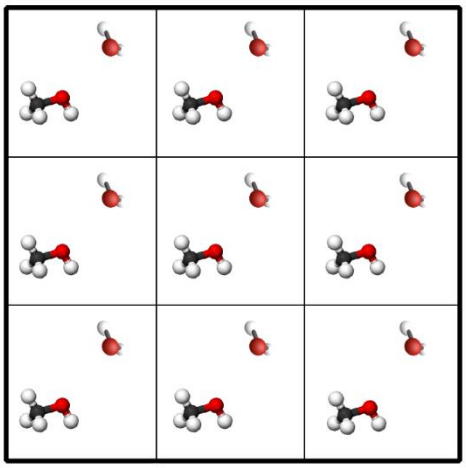

Figure 2.1: Representation of Periodic Boundary Conditions (PBC): the central box is replicated along the three dimensions

2.2.4 Potential energy minimization

A N-atoms system is defined by 3N cartesian coordinates and 3N-6 internal coordinates (bonds, angles and torsional angles), that's why the potential energy function is a complex multidimensional function. It can be represented by a surface called Potential Energy Surface (PES), of which every point describes a system configuration in space. This surface has some minimum points, each of one identifies a stable state: reached this stable state, the system will tend to maintain the corresponding configuration, being the near configurations at higher energy values. Several minimum points exist, and the lowest one is called *global minimum*. The aim of potential energy minimization is to lead the system configuration to one of these stable states before simulation starts, and in the ideal case to the state corresponding to the global minimum, with the purpose of avoid possible collapses during simulation due to high energy interactions. Two kind of methods exist to reach a minimum point of the PES: *derivatives* and *non-derivatives* methods. *First order derivatives methods* are Steepest Descent and Conjugate Gradient, in which the position of the minimum is identified by means of first derivative of the potential energy, namely the gradient. *Second derivatives methods* are Newton-Raphson and LBFGS, in which the second derivatives of the potential function are used to identify where the energy function change direction. Second derivatives methods are computationally more expensive but more accurate than first derivatives ones (Herman J. C. Berendsen 2007).

2.3 Molecular Dynamics

Molecular Dynamics (MD) is a computer simulation method useful to study the dynamic evolution of a system, like proteins or more complex biological systems. The system evolution in time is described through atom trajectories and therefore by their positions, velocities and forces. Trajectories can be obtained by solving Newton's equation of motion:

$$F_i = m_i \frac{\partial^2 r_i}{\partial t^2} \tag{10}$$

Taken the i^{th} particle of the system, m_i and r_i are respectively its mass and its position. Once trajectories are obtained it is possible to calculate system average properties.

Forces can be obtained in function of the Potential Energy:

$$F_i = -\frac{\partial U\,(r_i,\ldots,r_N)}{\partial r_i} \tag{11}$$

2.3.1 Statistical Ensemble

A system containing N atoms can be described by 6N coordinates, 3N coordinates of position and 3N coordinates of momentum (the product of the mass of the particle for its speed). Each set of 6N coordinates is a possible physical state of the system, also known as a microstate. All the possible physical states of the system are collected in a space, called *phase space*, of which every point is a system microstate. All the different microstates sharing the same macroscopic or thermodynamic state constitute a Statistical Ensemble.

Different kind of ensembles exist:

- The Micro-Canonical Ensemble (NVE), in which number of atoms (N), volume (V) and energy (E) are fixed. It is equivalent to an isolate system.
- The Canonical Ensemble (NVT), in which number of atoms (N), volume (V) and temperature (T) are fixed. It is equivalent to a closed system.
- The Grand Canonical Ensemble (μVT), in which chemical potential (μ), volume (V) and temperature (T) are fixed. It is equivalent to an open system.
- The Isobaric-Isothermal Ensemble (NPT): in which number of atoms (N), pressure (P) and temperature (T) are fixed.

The aim of MD is to obtain the macroscopic properties of the system, goal that is achieved by sampling the phase space and calculating the ensemble average of the property of interest. The ensemble average of property A is calculated by integrating as follows:

$$\langle A \rangle_{ensemble} = \iint dp^N \, dr^N A(p^N, r^N) \rho(p^N, r^N) \tag{12}$$

In which r is the atomic position, p is the momentum and $\rho\ (p^N, r^N)$ is the probability density function, defined as:

$$\rho(p^N, r^N) = \frac{1}{Q} \exp\left[-H(p^N, r^N)/k_b T\right] \tag{13}$$

k_b is the Boltzmann factor, H is the Hamiltonian, T is temperature and Q is the partition function.
The partition function is defined in function of the Hamiltonian:

$$Q = \iint dp^N \, dr^N \exp[-H(p^N, r^N)/k_b T] \tag{14}$$

The partition function is the sum of Boltzmann factors over all microstates and it relates microscopic thermodynamics variables to macroscopic properties. Anyway, an analytical solution of the previous expression doesn't exist because, in order to do this, all the possible states all the system should be known. With the aim to calculate the average property of interest, the *ergodic hypothesis* can be used, which states that for long enough periods of time the ensemble average and the time average are the equal.

$$\langle A \rangle_{ensemble} = \langle A \rangle_{time} \tag{15}$$

The ensemble average is defined as follows:

$$\langle A \rangle_{time} = \lim_{\tau \to \infty} \frac{1}{\tau} \int_{\tau=0}^{\tau} A(p^N\,(t), r^N\,(t)) dt \ \approx \frac{1}{M} \sum_{i=1}^{M} A(p^N, r^N) \tag{16}$$

t is time, M is the number of steps in the simulation and $A(p^N, r^N)$ is the instantaneous value of the analysed property. The number of steps need to be high enough to enable accurate sampling of the system.

2.3.2 Molecular Dynamics implementation scheme

As already mentioned, the aim of the molecular dynamics simulations is to obtain atom positions and velocities evolution in time, namely trajectories. In order to do this, Newton's equation of motion must be solved. Acceleration of each particle can be obtained by deriving potential energy with respect to particle position:

$$a = -\frac{1}{m}\frac{dV}{dr} \tag{17}$$

The potential energy is a very complex function of particle position, thus it can't be analytically solved and a numerical integration system must be used. Various integration methods and integration parameters can be chosen, and their choice must be sufficiently accurate so as to ensure proper phase state sampling. For example, a too big time step will cause instability and a too small time step will be useless and will only increase the computational cost: an appropriate time step is 1/10 of the period of the fastest harmonic oscillation. Verlet, Velocity Verlet and Leap-frog are some of the integration algorithms.

In Figure 2.2 it is shown a MD flowchart:

- Starting atomic positions are taken from initial structure, fox example a PDB file obtained from Protein Data Bank.
- Starting velocities are randomly assigned from Maxwell-Boltzmann distribution at a given temperature.
- Starting potential energy is calculated according to the chosen force field, and starting accelerations are obtained deriving potential with respect to particle positions.
- Thus, new positions and velocities are calculated, and step by step the same operations are repeated, providing the required trajectories.

After initial changes the system will reach an equilibrium, allowing for calculating the macroscopic thermodynamic properties by applying the ergodic hypothesis, thus calculating time averages of the proprieties of interest.

It is worth nothing that MD is a deterministic method: this means that starting with the same initial positions and same initial velocity distribution, the system evolution in time will always be the same in different simulations (Abraham et al. 2015; Hess et al. 2008; Van Der Spoel et al. 2005).

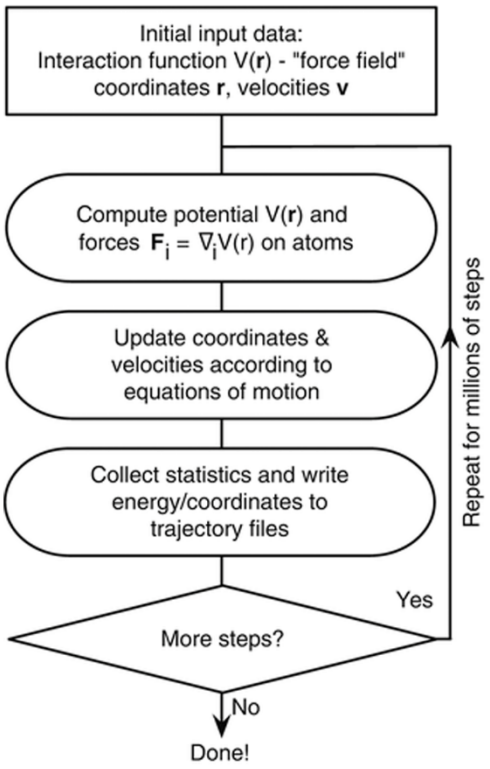

Figure 2.2: Molecular Dynamics algorithm scheme.
SOURCE:https://media.springernature.com/original/springer-static/image/chp%3A10.1007%2F978-1-4939-1465-4_1/MediaObjects/309033_2_En_1_Fig3_HTML.gif

2.3.3 Software package

Several MD codes for biomolecular simulation execution are available, like AMBER, CHARMM and GROMACS. In the execution of the work reported in this master thesis, AMBER and GROMACS software have been used. *GROningen MAchine for Chemical Simulations* (GROMACS) is free, open-source software under the GNU General Public License employed in simulations of biological systems like proteins, lipids, and nucleic acids, but also of non-biological systems, e.g. polymers (Abraham et al. 2015; Hess et al. 2008; Van Der Spoel et al. 2005). Its project began in 1991 at Department of Biophysical Chemistry, in the University of Groningen and now continues thanks to universities and research centres around the world. It is written in C and C++ language and works on Unix-like operating systems, like Linux, macOS, Windows.

Assisted Model Building with Energy Refinement (AMBER) is another molecular dynamics software package that simulates native AMBER force fields for molecular dynamics of biomolecules (Sprenger, Jaeger, and Pfaendtner 2015; Pearlman et al. 1995; Case et al. 2005). The force field was originally developed by Peter Kollman's group at the University of California, San Francisco. The software is written in Fortran 90 and C programming languages and works with most major Unix-like operating systems and compilers. It is made up of several programs. In this work the programs used are:

- LEaP: prepares input files for the simulation programs, providing coordinates, parameters and topologies.
- Antechamber: allows for parameterizing small organic molecules using *Generalized Amber Force Field* (GAFF).

3 Biological Background

In this chapter a brief explanation of microtubule structure and functions is provided.

3.1 Introduction

Microtubules are cytoskeleton filaments made up of αβ-tubulin heterodimers (Huzil et al. 2007) arranged in head to tail fashion (Stanton et al. 2011), playing very important and indispensable roles in eukaryotes cells. They form the cytoskeleton together with actin filaments and intermediate filaments, and all together they provide the cell with the appropriate spatial and structural organization. Within the cytoskeleton filaments, the microtubule (MT) exhibits the significantly highest bending stiffness, which depends on the mechanical properties and intermolecular interactions of the tubulin dimers (Deriu et al. 2010). Microtubules also play critically important roles in transport, migration (Mitra and Sept 2008), maintenance of cell polarity (Bennett et al. 2009), mitosis (during which microtubules segregate and separate the chromosomes), in transport of vesicles, cell signalling, cell shaping and sensory transduction (Kumbhar et al. 2016), positioning of cellular organelles and cellular motility (Santoshi and Naik 2014). The central role played by microtubules in cell division (the segregation of chromosomes) makes them a desirable target for cancer chemotherapy (Santoshi and Naik 2014). Many of these functions require that microtubules dynamically assemble and disassemble (Mitra and Sept 2008).

3.2 Tubulin structure

Microtubules are hollow, cylindrical polymers formed from the self-association of tubulin into linear protofilaments (Mitra and Sept 2008). Tubulin is a heterodimer of α and β-tubulin, two forms of tubulin that have 40% sequence homology and highly similar tertiary structures (Mitra and Sept 2008). Each tubulin is 55 kDa heavy and can be divided into the three functional domains: the Rossman fold, namely the N-terminal domain (1–205) containing the nucleotide binding region, the intermediate domain (206–381), and C-terminal domain (residue 440 for α-tubulin and residue 427 for β-tubulin) (Kumbhar et al. 2016; Deriu et al. 2010). The N-terminal domain (the nucleotide-binding domain) of each monomer consists of six parallel β-strands (S1-S6) alternating with helices (H1-H6). Those strands and helices are linked by 6 loops (loops T1-T6), directly involved in the binding with nucleotide. The N-terminal end of the core helix H7 also contribute to the nucleotide binding. This core helix joins the nucleotide binding domain with the second domain, consisting of three helices (H8-H10) and beta sheet (S7-S10). Two more antiparallel helices (H11-H12) constitute the C-terminal region, crossing over the previous two domains.

Monomer shapes are highly complementary to the interface within the dimer (Löwe et al. 2001). Within the microtubule, interactions between adjacent dimers are exerted through lateral and longitudinal noncovalent bonds (VanBuren, Odde, and Cassimeris 2002). Those lateral and longitudinal interactions are different: lateral contacts between two equal subunits α-α or β-β are mainly electrostatic, while longitudinal α-β interactions are mostly hydrophobic. Moreover, lateral contacts are weaker than longitudinal ones (Pampaloni and Florin 2008). Structures involved in longitudinal interactions are T7 loop, M-loop (the loop between S7 and H9)(Löwe et al. 2001) and H10 helix (Deriu et al. 2010), while structure involved in lateral contacts are H4-H5 loop, M-loop, which interacts with H1-S2 loop and H3 helix (Löwe et al. 2001), and H10 helix (Deriu et al. 2010). Generally, tubulin monomers are proteins with a very stable central core composed of sheets, while external surfaces are mainly composed by high flexible loops (as H1-S2 loop) and α-helices (Deriu et al. 2010). In MTs, protofilaments join laterally to form a hollow cylinder of about 25 nm diameter. The number of protofilaments in a MT usually vary between 9 and 16 and the most common structure is made up of 13 protofilaments (Pampaloni and Florin 2008). MTs can differ not only in the number of protofilaments, but also in the helical pitch, namely the number of monomers at which the helix closes (Pampaloni and Florin 2008), as shown in Figure 3.1.

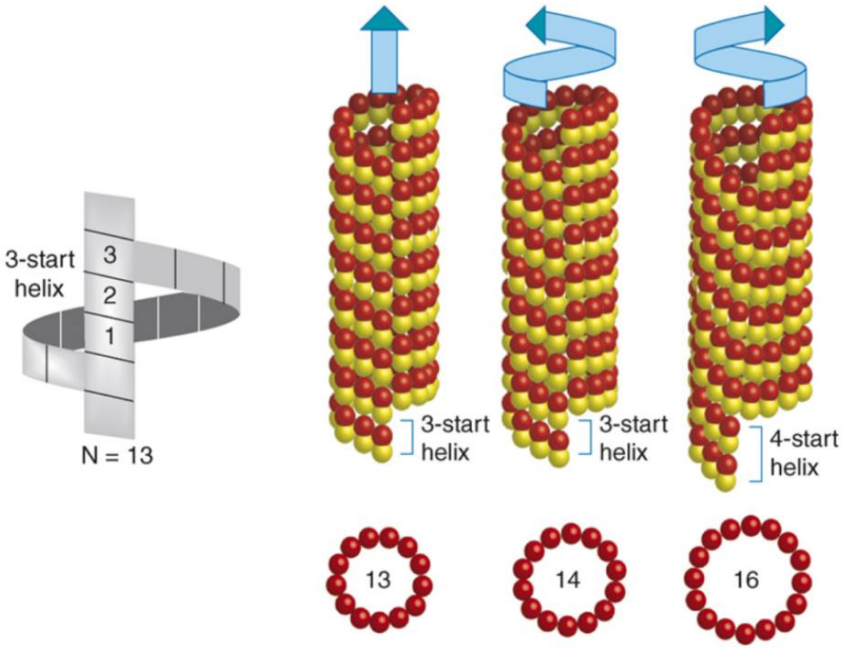

Figure 3.1: MTs architecture.

Pampaloni, F., & Florin, E.-L. (2008) doi:10.1016/j.tibtech.2008.03.002

MTs architecture is simply identified specifying the number of protofilaments and the pitch: for example, 13:3 indicates a 13 protofilaments MT with a pitch of 3 monomers. It has been demonstrated that MTs bending lead to a lateral shift between two adjacent protofilaments, of about 0.2 nm. Consequently, bonds along the protofilaments are stretched and these stresses are relaxed though twisting of protofilaments along MT's axis, leading to the formation of MTs with different number of protofilaments (Pampaloni and Florin 2008).

3.3 Microtubule polymerization

MTs are polar systems characterized by different polarity in the two ends causing a different growth rate in the two terminal parts: the α-tubulin is exposed to the minus end, the one with the slowest growth, while β-tubulin is exposed to the plus end, characterized by the faster growth. α-tubulin binds a GTP molecule into a non-exchangeable nucleotide binding site, placed at the monomer-monomer interface within the dimer (Löwe et al. 2001). After the α-tubulin binds to the β-tubulin, another GTP molecule binds the β-tubulin, in the exchangeable site, which lies on the dimer surface and touches the α-tubulin of a subsequent dimer, leading to the formation of the protofilament. GTP bound to β-tubulin, being exposed unlike GTP bound to α-tubulin, can hydrolyse resulting in GDP, and the addition of new tubulin dimers converts this site from exchangeable to non-exchangeable (Rendine, Pieraccini, and Sironi 2010). Each monomer of tubulin binds GTP in analogous locations (Bennett et al. 2009), and hydrolysis in β-tubulin is thought to lead to conformational changes in the dimer, giving the structure enough flexibility to allow for polymerization-depolymerization cycles, the so-called dynamic instability (Huzil et al. 2007). Indeed GDP-tubulin is more unstable than GTP-tubulin in lattice, and because of this enhanced instability, the plus end of a growing microtubule is protected though a so called GTP-cap, tubulins bound to GTP instead of GDP, preventing microtubule to undergoes depolymerization. Dynamic instability is relevant only at the plus end of MT, because minus end is usually capped by other proteins, like for example centrosome, and depolymerizes only when un-capped and free in the cytoplasm. So usually the minus end is anchored to the centrosome, while the plus end fluctuates in the cytoplasm searching for binding (Desai and Mitchison 1997). Unpolymerized αβ-tubulin dimers are characterized by a bent conformation, which switches to a straight conformation during microtubule polymerization (Tripathi et al. 2018). Two mechanism model about how this happens are proposed, the lattice and the allosteric model, and they will be explained later. This bending happens around an "anchor point" located at the intradimer interface that stands still during the conformational change. This anchor point involves hydrophobic interactions between the H8 helix of β-tubulin and the surface of α-tubulin (Igaev and Grubmüller 2018). In the

microtubules, conformational movements like twisting (firstly) and bending in/between α and β-tubulin seem to be very important for maintaining straight αβ-tubulin dimer conformation (Figure 3.2). Indeed, for example, twisting motion contributes in maintaining lateral contacts (Tripathi et al. 2018).

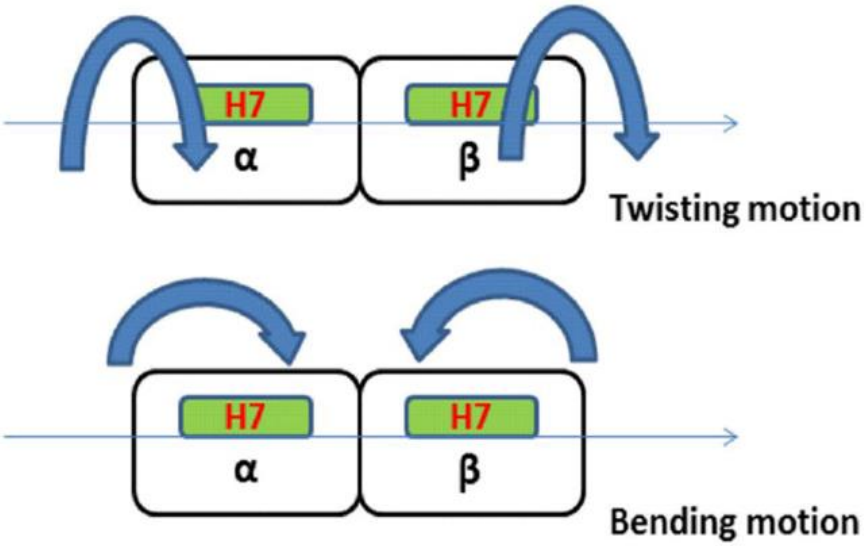

Figure 3.2: twisting and bending motion of tubulin dimers.
Tripathi, S., Srivastava, G., Singh, A., Prakasham, A. P., Negi, A. S., & Sharma, A. (2018) doi:10.1007/s10822-018-0109-y

3.3.1 Microtubule Instability

MT functionality is closely linked to its polymerization dynamics at the plus end (the one with exposed β-tubulin), which alternates between growth and disassembly phases (Mitchison and Kirschner 1984). Assembly and disassembly are regulated by temperature, pH and ionic concentrations sensitive mechanisms. The stabilization of the whole structure of the MT is normally guaranteed by the fixing of a GTP cap to the end of the MT, which protects the terminal β tubulin from a conformational change that is then thought to induce its dissociation (Huzil et al. 2007). In disassembly conditions microtubules show coiled ends, as if the protofilaments separate and unroll from the microtubular structure (Mandelkow, Mandelkow, and Milligan 1991). MTs transition from assembly to disassembly state is called *catastrophe*, and this happens when the GTP cap of MT is lost. Conversely, *rescue* is the transition from disassembly to assembly and occurs with the re-establishment of the tubulin-GTP cap (VanBuren, Odde, and Cassimeris 2002). Free tubulin requires guanosine triphosphate (GTP) to start the formation of new MTs (nucleation) and extend already existing ones (growth). MTs grow constantly till the GTP hydrolysis in the

lattice is slower than the arrival of new dimers, creating the so-called GTP cap at the MT tip. If GTP hydrolysis gets faster than MT growth, the MT lattice depolymerizes fast. This catastrophe is resisted by the rescue mechanism, made possible thanks to GTP-dimers spots embedded in the depolymerizing MT lattice, working as nucleation checkpoints (Igaev and Grubmüller 2018). GDP-tubulin released during disassembly exchanges GDP for GTP and becomes ready again for polymerization and nucleation. Analysis of electron microscopy images of MTs and structural data showed that tubulin dimers are straight when embedded in the MT lattice, not very kinked (about 5° per dimer) at the tips of growing MTs, and highly bent outwards (about 12° per dimer) at the tips of MT in disassembly phase (Igaev and Grubmüller 2018). It is thus possible that tubulin straightening takes place during polymerization, while highly kinked conformations are assumed in depolymerized GDP-tubulin (Igaev and Grubmüller 2018). This conformational change, from straight to curved, is thought to be responsible of destabilization. However, it is not certain whether this transformation is due to the nucleotide state or to the lateral and longitudinal contacts in the microtubule lattice (Grafmüller and Voth 2011). Two different theories have been proposed:

- According to the *allosteric model*, the GDP-tubulin is characterized by a curved structure at the intradimer interface, between α and β subunits, while the GTP-tubulin is characterized by a straight structure (Bennett et al. 2009). Free tubulin dimers bind GTP prior to assembly, which causes a bent-to-straight conformational change, making possible dimer integration into the MT lattice (Igaev and Grubmüller 2018). The presence of structures at the microtubule growing ends which need a nearly straight conformation supports this theory. Some studies based on molecular dynamics simulation show a greater bending for GDP-tubulin, probably due to an increase in flexibility in the intradimer region, causing conformational instabilities in the vicinity of the E-site in the β-tubulin, which could lead to disassembly once the GTP-cap gets lost (Bennett et al. 2009).
- Alternatively, the *lattice model* affirms that both GTP and GDP free tubulin has a bent conformation, and tubulin dimer assumes a straight conformation only after integration into the MT lattice, and does not depend on GTP binding (Igaev and Grubmüller 2018). Here, GTP tubulin provide better lattice contacts, straightening an incoming dimer reducing the energy barrier (Bennett et al. 2009). Many molecular dynamics (MD) studies have been done to understand more about this behaviour, and many of them support the lattice model (Igaev and Grubmüller 2018).

Contrary to both allosteric and lattice models, Igaev et al. (2018) affirm that GTP-tubulin can take different degrees of curvature, unlike GDP-tubulin, which is less able to explore different conformations and it is

characterized by a higher stiffness (Igaev and Grubmüller 2018). By their new purposed model, GTP binding does not force tubulin to assume a straight structure, but it simply enhances its flexibility compared to GDP, thus making easier the lattice effect, namely the dimer straightening upon integration in MT wall. This enhanced flexibility leads to a more relaxed structure in assembled MT wall, thus to a greater stability of the system compared to the one constituted by GDP tubulin. Additionally, in MD simulations starting with a straight structure the system quickly moved to a kinked conformation, demonstrating that GTP-tubulin has not a straight structure and identifying kinked conformation as the more relaxed one. However, it is not yet clear which of the proposed models is the correct one, and the debate is still open.

3.4 Tubulin Crystal Structures

Protein Data Bank (PDB) is an archive, providing a collection of data and 3D structures about proteins, nucleic acids, and complex assemblies. Its project started in 1971, and till today several crystallographic structures had been added to the archive, available to anyone from RSCB PDB web site. The first tubulin structure, 1TUB (1998), was crystallized as a flat Zn^{2+} induced sheet using docetaxel as a stabilizing agent. 1FFX (2000) was obtained using a stathmin-like domain. This structure was later improved and uploaded as 1JFF (2001), and paclitaxel was used as a stabilizing agent. Later 1TVK (2004) was released, with epothilone A as stabilizing agents, bound to the taxane binding site. 1SA0 and 1SA1 (2004) were obtained with a higher resolution, with Colchicine and podophyllotoxin respectively bound. Later 1Z2B (2005) was introduced, bound with both Colchicine and vinblastine (Desai and Mitchison 1997). Two more additional structures have been included in the database, 3J6E and 4O2B (2014). The former is a portion of the microtubule wall, constituted by 6 tubulin dimers, stabilized by GmpCpp, the latter is a tetramer, a Stathmin-4 and a tubulin-tyrosine ligase.

3.5 Isotypes

In vertebrates' cells, 6 and 10 isotypes of α and β tubulins are present, respectively (Pepe et al. 2009; Huzil, Ludueña, and Tuszynski 2006). Isotypes differ from each other in the amino acid sequence, with most of the differences occurring in the extreme carboxy terminal region (residue 430 and greater)(Huzil et al. 2007), in the last 15 to 20 C-terminal amino acids, probably the binding sites for many microtubules associated proteins (MAPs)(Kumbhar et al. 2016), with 90% of similarity among isotypes (Massarotti et al. 2012). That's why the C-terminal region has been used to identify the various β-tubulin isotypes.

Tubulin isotypes are important in regulating microtubule dynamics, and they are specifically expressed to properly regulate microtubule assembly/disassembly cycle (Huzil et al. 2007). In the human species, the ten types of β-tubulin are: βI, βIIa/b, βIII, βIVa/b, βV, βVI, βVII and βVIII (Huzil, Ludueña, and Tuszynski 2006). β-tubulin, among the two tubulin subunits, is the mainly involved in binding with drugs, and this is the reason why most of the attention has been focused on it during years.

Isotypes are expressed in different quantities in the various human tissues. For example, βI-tubulin is the most abundant isotype, βIII had been found only in neuronal tissues and testis (Huzil et al. 2007), βIVa is found in neuronal and glial cells and βVI is expressed in blood, bone marrow and spleen etc (Kumbhar et al. 2019). The Figure 3.3 describes in detail the expression of the different types of human tubulin in the various tissues:

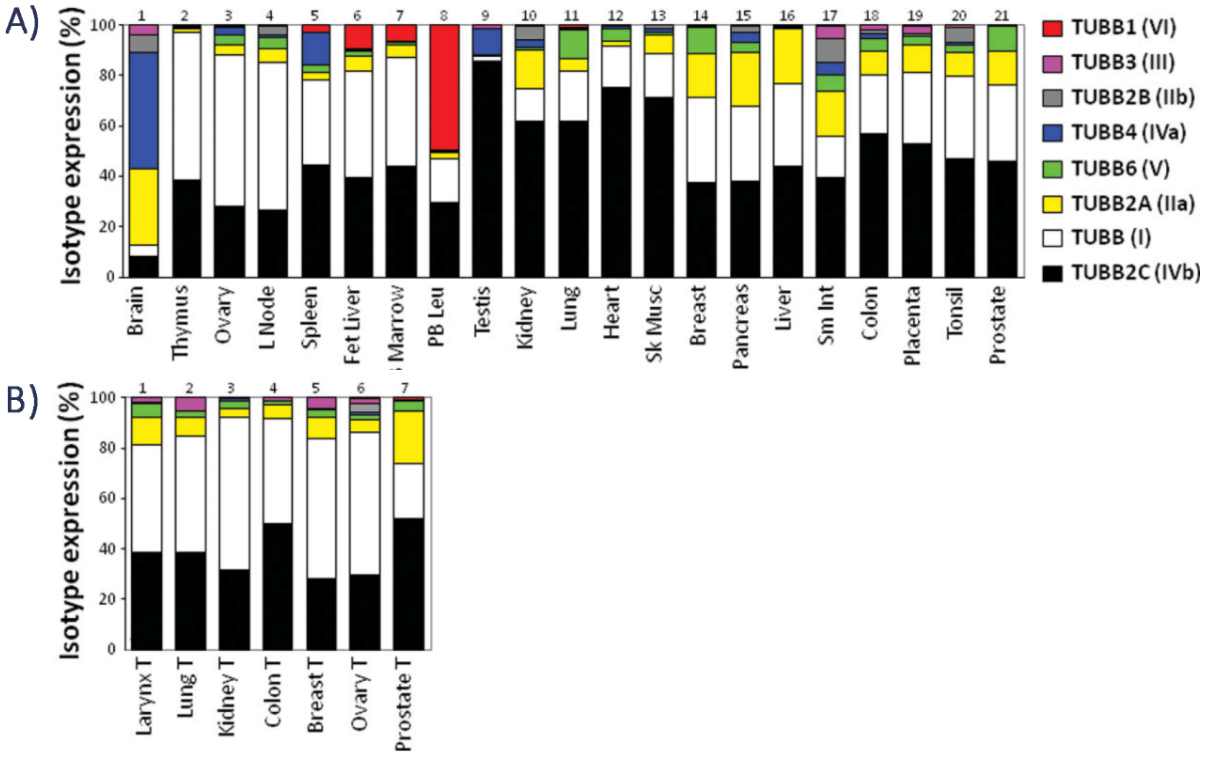

Figure 3.3: expression level of eight human isotypes in healty (A) and cancer (B) cells.
Leandro-García, L. J., Leskelä, S., Landa, I., Montero-Conde, C., López-Jiménez, E., Letón, R., Rodríguez-Antona, C. (2010) doi:10.1002/cm.20436

Anyway, tubulin isoform expression is not only related on cell type or tissue, but also on external factors such as anticancer therapy, which lead to a change in the expression of isotypes following the administration (Massarotti et al. 2012).

Although sequence alignment shows that many of the differences between isotypes occur outside the main drug binding sites, in residues involved in protein-protein interactions (Huzil et al. 2007), tubulin isotypes have different binding affinities for various anti-cancer agents (Kumbhar et al. 2016). This causes the different affinity of drugs for different types of tissue and cells (Santoshi and Naik 2014), contributing in the development of drug resistance (Kumbhar et al. 2016). As an example, overexpression of βIII in cancer cells such as ovarian, breast and non-small-cell lung cancer probably causes resistance to paclitaxel. Overexpression of class βV in cancer cells probably causes resistance to taxane (Santoshi and Naik 2014). Cancer cells particularly express isotypes that are not expressed in healthy tissue (Santoshi and Naik 2014). However, this aspect could be favourable since targeting an isotype mostly expressed by cancer cells increases specificity by decreasing side effects and damage to healthy tissues (Huzil, Mane, and Tuszynski 2010). Anyway, mechanisms leading to drug resistance because of the expression of certain isotypes are still not well understood.

3.6 Microtubule Targeting Agents

Microtubule targeting agents (MTAs) are molecules able to bind microtubules, altering their dynamics and causing mitotic arrest of dividing cells. MTAs can alter mitosis because MTs form the mitotic spindle: its assembly failure leads to mitotic arrest, apoptosis, and eventually cell death. For this reason, MTAs are widely used in cancer therapy (Stanton et al. 2011).

Tubulin-binding drugs interact mostly with β-tubulin (Huzil et al. 2007), by binding three distinct sites viz., *Taxol*, *Colchicine* and *Vinca* site (Figure 3.4). Those molecules can interfere with assembly or disassembly of microtubules both by over-stabilizing and destabilizing them:

- Vinca and Colchicine binding agents (also called Colchicine site inhibitors CSIs) are destabilizing agents, and both bind to curved free tubulin.
- Taxol targeting agents binds to the polymerized microtubules stabilizing it; thus, they bind tubulin in a straighter conformation (Kumbhar et al. 2019).

Taxol and vinblastine drugs are used in clinical oncology, while Colchicine agents are still unused (Massarotti et al. 2012).

Most drugs bind tubulin of both healthy and unhealthy cells, resulting into a series of side effects that decrease their effectiveness (Huzil et al. 2007). Moreover, cancer cells develop mechanisms of drug-resistance after prolonged administration of anticancer drugs, thus decreasing their sensitivity to the drugs. In this cases, more aggressive therapies, with increased doses, are required to obtain the same effects, consequently enhancing the side effects and the toxicity towards healthy tissues (Pepe et al. 2009). The expression of tubulin isotypes βI, βII, βIII, βIVa, and βV in cancerous cells is connected to multidrug-resistance (Kumbhar et al. 2019), but a complete understanding of the mechanisms that cause drug resistance is of fundamental importance for the design of new more effective drugs.

Huzil et al. (2006) (Huzil, Ludueña, and Tuszynski 2006) analysed ten human β tubulins focusing on differences among Taxol, Colchicine and Vinca binding sites.

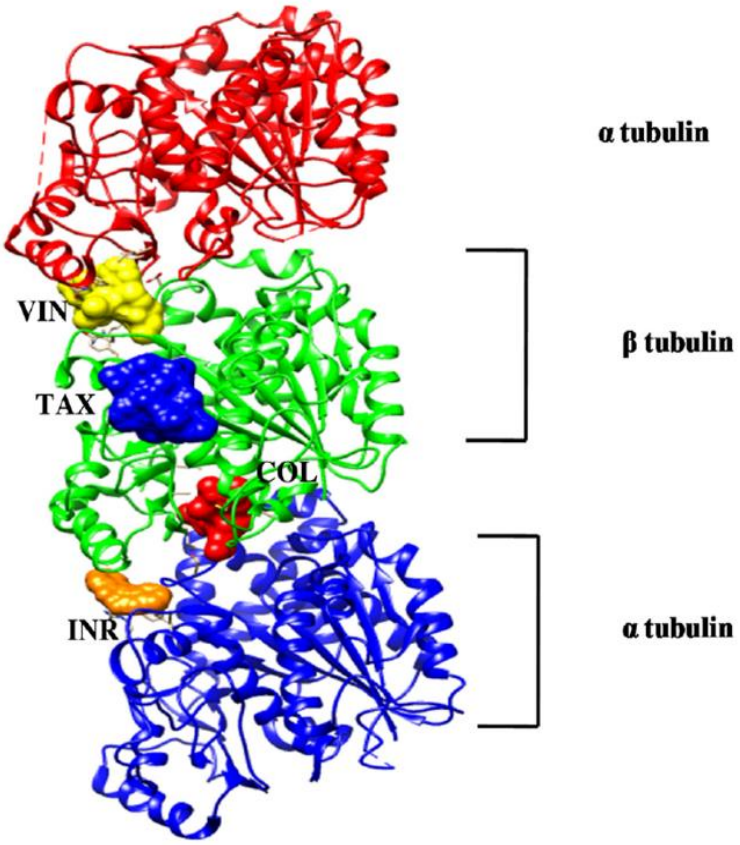

Figure 3.4: vinca, Taxol and Colchicine binding sites.

Mohan, L., Raghav, D., Ashraf, S. M., Sebastian, J., & Rathinasamy, K. (2018) doi:10.1016/j.biopha.2018.05.127

3.6.1 Taxol

Taxol (or Paclitaxel) (Figure 3.5) is a widely used drug in the treatment of ovarian cancer, breast cancer, melanoma, non-small cell lung cancer and Kaposi's sarcoma. Taxol binds the β-tubulin dimer leading to the stabilization of microtubules against depolymerization induced by Ca^{2+}, cold, and dilution (Mitra and Sept 2008). Taxol binding site is localized in β-tubulin, more specifically in the microtubule lumen, near the interface between lateral protofilaments. It is made up of helix H7, strand S7, loop H6-H7, loop S7-H7 (also known as M-loop) and loop S9-S10 of β-tubulin (Prota et al. 2013). Being a microtubule stabilizing agent, its effect is to alter the MT dynamic instability by making easier microtubules assembly, inhibiting cell mitosis preventing entry into the anaphase, in which replicated chromosomes are split and the new daughter chromatids are moved to opposite poles of the cell (Mitra and Sept 2008). The effect of agents such as Taxol and other stabilizing agents is such that they promote polymerization when it cannot occur spontaneously (Prota et al. 2013).

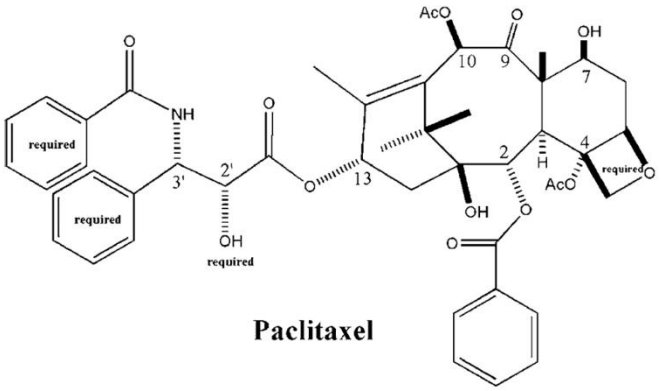

Figure 3.5: Paclitaxel.

Xu, S., Chi, S., Jin, Y., Shi, Q., Ge, M., Wang, S., & Zhang, X. (2011) doi:10.1007/s00894-011-1083-7

Taxol mechanism of action can be explained as follows: it increases flexibility of tubulin dimer, which can consequently better tolerate the conformational changes due to possible curvatures of the protofilament (Mitra and Sept 2008). In addition, it changes M-loop position, improving interactions with the dimer located in the adjacent protofilament. In this way microtubule structure is stabilized (Mitra and Sept 2008).

3.6.2 Colchicine

Colchicine and Colchicine site inhibitors (CSIs) are a class of destabilizing microtubule binding agents acting on the α and β-tubulin interface, in the Colchicine binding site (CBS)(Tripathi et al. 2018). CBS is constituted, in the β-tubulin, by S9 (Val351–Cys356) and S8 (Leu313–Aeg320) sheets, H7 (Tyr224–Arg243) and H8 (Leu252–Val260) helices, and T7 loop (Phe244–Asp251) and by αT5 loop (αPro173–αVal180) in the α-tubulin (Tripathi et al. 2018) (Figure 3.6). They are also the regions mainly involved in maintaining the straight and bent conformation of αβ-tubulin dimer (Kumbhar et al. 2019).

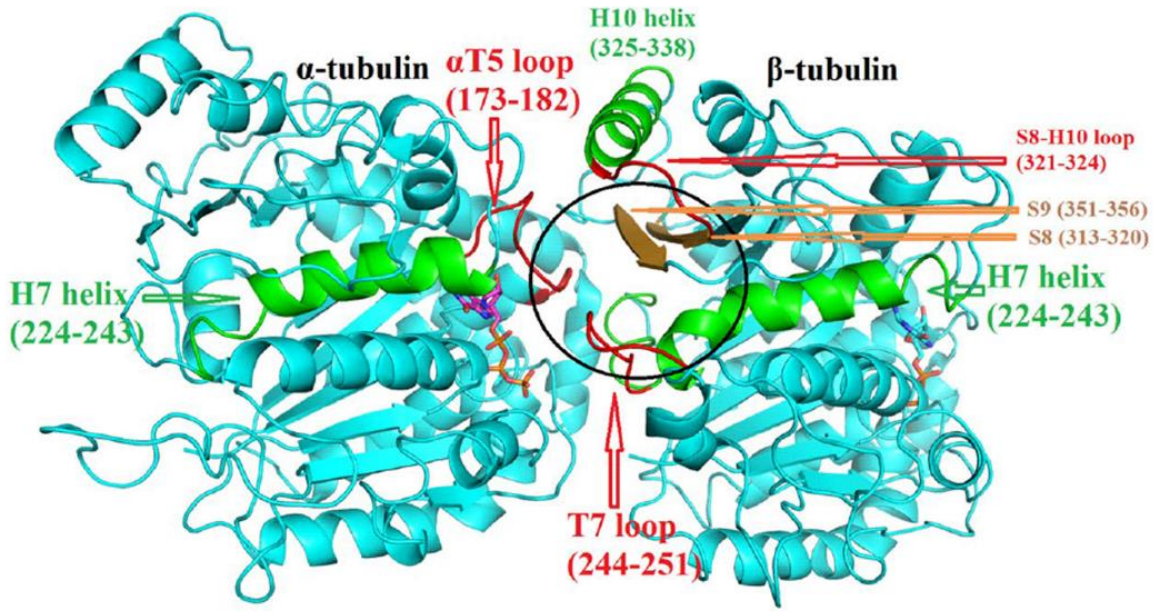

Figure 3.6: colchcine binding site.

Tripathi, S., Srivastava, G., Singh, A., Prakasham, A. P., Negi, A. S., & Sharma, A. (2018) doi:10.1007/s10822-018-0109-y

In the straight conformation, β-tubulin regions S9 and S8 sheets, H7 and H8 helices, and T7 loop align to the α-tubulin (Figure 3.7). In the bent conformation, the relative positions among the same regions change (Tripathi et al. 2018).

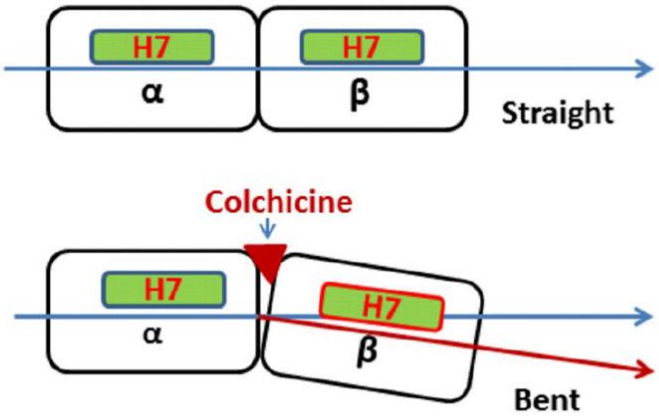

Figure 3.7: straight and bent conformation.

Tripathi, S., Srivastava, G., Singh, A., Prakasham, A. P., Negi, A. S., & Sharma, A. (2018) doi:10.1007/s10822-018-0109-y

Colchicine (Figure 3.8) was extracted for the first time from the leaves of meadow saffron, and since the 18th Century it has been used in the treatment of gout (Löwe et al. 2001). Colchicine is composed of three rings i.e. trimethoxy benzene ring (A ring), methoxytropone ring (C ring), and a seven member ring (B ring) with acetamido group at C7 position. Although Colchicine is more buried in β-tubulin, the B ring side chain mostly interacts with α-tubulin (Botta et al. 2009).

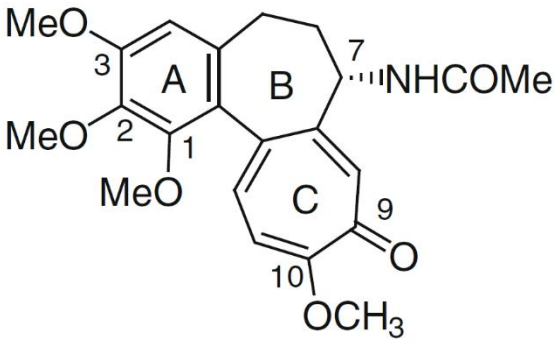

Figure 3.8: Colchicine chemical structure.

Botta, M., Forli, S., Magnani, M., & Manetti, F. (2008)doi:10.1007/128_2008_20

It is known that unpolymerized αβ-tubulin dimer has bent conformation, while polymerized αβ-tubulin dimer acquires straight conformation: Colchicine site binding drugs first bind to the free αβ-tubulin dimer

and then this tubulin-drug complex gets incorporated into the microtubule, preventing αβ-tubulin dimer from adopting straight conformation also in the polymerized microtubule (Tripathi et al. 2018). Furthermore, CSIs disturb twisting and bending conformational motions of αβ-tubulin dimer, essential in reaching straight conformation and maintaining lateral contacts in MT lattice. In this way microtubule destabilization action is exerted (Kumbhar et al. 2019; Tripathi et al. 2018).

Several papers dealing with the Colchicine mechanism of action have been published. Dorléans et al. (2009) (Dorléans et al. 2009), Barbier et al. (2010) (Pascale Barbier et al. 2010), Prota et al. (2014) (Prota et al. 2014) agree on the following mechanism: all those studies reveal that the unliganded complex is curved exactly like the Colchicine-bounded one: the only structural differences are local differences and they involve above all the T7 loop, the loop connecting helix H8 to helix H7. In the unliganded complex, this loop occupies the Colchicine binding site, releasing it only in the presence of the drug: T7 loop translates going from the straight to curved conformation, as shown in Figure 3.9. Barbier et al. (2010) describes additional structural changes (Figure 3.9). In straight conformation, strands S8 and S9 get closer to helix H8, and together with the H7 translation they restrict the Colchicine binding site. The transition from curved to straight structure is thus allowed only in the absence of any ligand in the Colchicine binding site: because of steric hindrance, a drug in this site would prevent all the movements necessary to achieve the straight conformation, counteracting the polymerization process in which the achievement of the straight conformation is fundamental.

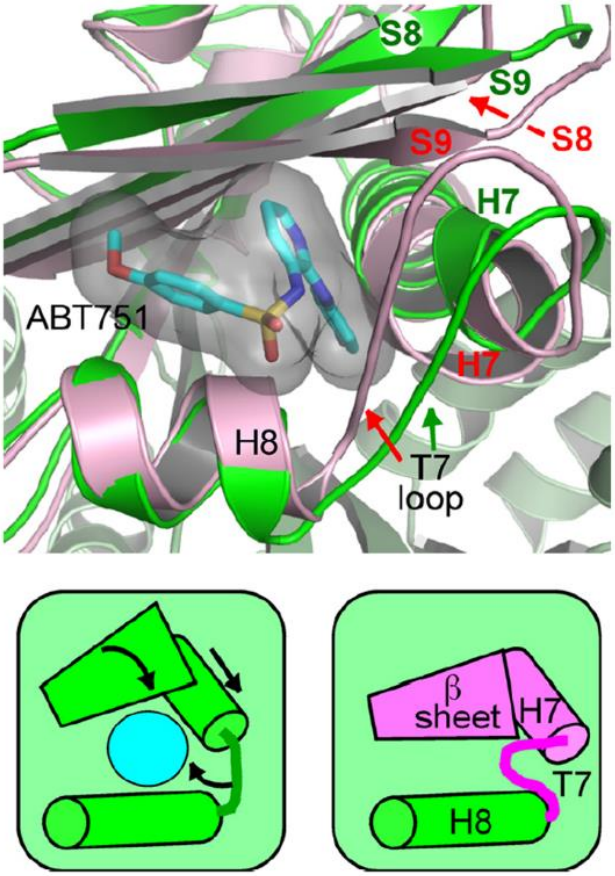

Figure 3.9: structural changes from curved (green) to straight (pink) structure in Colchicine binding site. Dorleans, A., Gigant, B., Ravelli, R. B. G., Mailliet, P., Mikol, V., & Knossow, M. (2009) doi:10.1073/pnas.0904223106

3.6.3 Vinca Alkaloids

Vinca alkaloids are indole alkaloids extracted from Chataranus roseus, widely used as anticancer agents thanks to their ability to inhibit tubulin polymerization. Vinca alkaloids binding site has been defined in 2005 thanks to x-ray diffraction of tubulin complexed with vinblastine and other compounds (PDB entry: 1Z2B)(Botta et al. 2009). This tubulin has a curved structure and vinblastine binds at the interface between two different dimers, preferentially at the plus end of the microtubule (P. Barbier et al. 2014). More specifically the binding site is made up of loop T7, helix H10 strand S9 of α-tubulin and H6, loop T5 and loop H6-H7 of β-tubulin. Obviously, the region in which Vinca alkaloids bind tubulin is involved in longitudinal contacts within protofilaments. The mechanism of action of this class of compounds consist

in introducing a curvature in dimer-dimer interface. In Figure 3.10, the residues involved in the binding are represented in blue, with vinblastine in green (Botta et al. 2009).

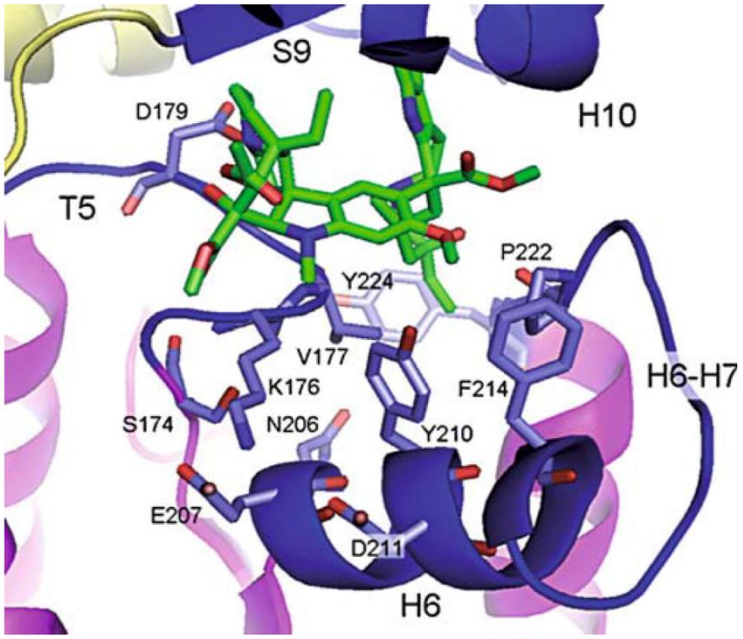

Figure 3.10: vinblastine (green) in its binding site.
Botta, M., Forli, S., Magnani, M., & Manetti, F. (2008) doi:10.1007/128_2008_20

Corderch et al. (2012) (Coderch, Morreale, and Gago 2012) defined the tubulin residues involved in interaction with four Vinca alkaloids: vinblastine, vincristine, vinorelbine and vinflunine. In the β-subunit, residues involved in binding are Val177, Tyr210, Thr221, Pro222, Thr223, Tyr224 and Leu227, Pro175 and Lys176, while in the α-tubulin they are Leu248, Val328, Asn329, Ile332, Ala333 and Val353.

Devred el al. (2008) (Devred et al. 2008), revealed that vinblastine can increase stathmin activity (promoting depolymerization) and vice versa. So, this constitutes one of the possible mechanisms of action of vinblastine. Moreover, Vertessy et al. (1998)(Vertessy et al. 1998) showed that Vinca alkaloids can bind to the universal calcium signal transductor, calmodulin (CaM), affecting the interaction of CaM with its targets, some of which are involved in MT regulation, like MAP6, able to stabilize microtubule in a calcium-dependent manner. Thus, Vinca alkaloids can affect MT stability not only though direct binding but also though indirect effects.

4 Molecular modelling to investigate tubulin conformational dynamics driven by antimitotic agents

4.1 Abstract

Microtubules (MT) play key roles in cell mitosis and in particular they help to segregate chromosomes. For this reason, MT are a desirable target in cancer treatment for the inhibition of the unregulated tumoral cells division. In addition, several tubulin isotypes exist, each one having its own sensitivity to a specific drug and a different level of expression depending on tissues. This represents an important opportunity in drug design, which exploits the isotypes expression to study and synthesize highly specific drugs, having a greater affinity only for diseased cells and causing reduced systemic effects. Antimitotic drugs act by interfering with MT polymerization-depolymerization kinetics, but the molecular mechanisms responsible for the drug activity is still unclear. These drugs can be classified according to their effects on MT dynamics. In this work, we have considered one stabilizing agent, i.e. Taxol, and a destabilizing one, i.e. Colchicine. More in detail, molecular modelling has been employed to investigate the effects of these drugs on the conformational behaviour expressed by two different human tubulin isotypes. Results of the present research might shed light on the molecular mechanism of action of investigated drugs and thus make clearer the induced tubulin conformational modifications which affect the entire MT dynamics.

4.2 Introduction

Microtubules (MTs), together with actin filaments (F-actin) and intermediate filaments (IFs), form the cellular cytoskeleton, providing the cell with the appropriate spatial and structural organization. Microtubules also play critically important roles within the cell, i.e. in transport, migration (Mitra and Sept 2008), maintenance of cell polarity (Bennett et al. 2009), cell signalling and mitosis, during which they separate the chromosomes forming the mitotic spindle (Kumbhar et al. 2016). Since cancer cells proliferate by unregulated cell divisions, the central role played by microtubules in cell division makes them a desirable target for cancer chemotherapy (Santoshi and Naik 2014). In this context, MT functionality is hindered by the alteration of their dynamic polymerization equilibrium (Mitra and Sept 2008).

MT are hollow, cylindrical polymers formed from the self-association of tubulin into linear protofilaments (Mitra and Sept 2008). Tubulin is a heterodimer of α and β-tubulin. The α-tubulin binds a GTP molecule into a non-exchangeable nucleotide binding site, placed at the monomer-monomer interface within the dimer (Löwe et al. 2001). Following formation of the tubulin dimer, another GTP molecule bounded to the β-tubulin in the exchangeable site can hydrolyse resulting in GDP (Löwe et al. 2001). Each monomer of tubulin binds GTP in analogous locations (Bennett et al. 2009) and GDP-tubulin is more unstable than GTP-tubulin in the lattice (Huzil et al. 2007). For this reason, the plus end of a growing microtubule is protected by the so called GTP-cap, namely tubulins bound to GTP instead of GDP, which prevents microtubule disruption. MTs transition from assembly to disassembly state is called *catastrophe* and it happens when the GTP cap of MT is lost. Conversely, *rescue* is the transition from disassembly to assembly and occurs with the re-establishment of the tubulin-GTP cap (VanBuren, Odde, and Cassimeris 2002). Moreover, tubulin dimers are straight when embedded in the MT lattice and highly bent at the tips of MT in disassembly phase. It is thus possible that tubulin straightening takes place during polymerization, while highly kinked conformations are assumed during depolymerization (Igaev and Grubmüller 2018). However, it is not certain whether this conformational switch, from straight to curved, is due to the nucleotide state or to the lateral and longitudinal contacts introduced in the lattice (Grafmüller and Voth 2011). In fact, according to the *allosteric model*, the GDP-tubulin has a curved shape, while the GTP-tubulin is characterized by a straight structure (Bennett et al. 2009): free tubulin dimers bind GTP prior to assembly, which causes a bent-to-straight conformational change, making possible dimer integration into the MT lattice. Alternatively, the *lattice model* affirms that both GTP and GDP free tubulin has a bent conformation, regardless of the nucleotide state, and tubulin dimer assumes a straight conformation only after integration into the MT lattice (Igaev and Grubmüller 2018).

Microtubule targeting agents (MTAs) are molecules able to bind microtubules, altering their dynamics and causing mitotic arrest. Tubulin-binding drugs interact mostly with β-tubulin (Huzil et al. 2007), by binding three distinct sites viz., *Taxol*, *Colchicine* and *Vinca* site. Those molecules can interfere with assembly or disassembly of microtubules both by over-stabilizing or destabilizing them: Vinca and Colchicine are destabilizing agents, while Taxol is a stabilizer. Vinca and Colchicine act by binding to curved free tubulin, introducing a curvature in the dimer-dimer and intra-dimer interface, respectively (Kumbhar et al. 2019; Botta et al. 2009), preventing αβ-tubulin dimer from adopting straight conformation also in the polymerized microtubule. Taxol, instead, binds to the polymerized microtubules, making easier their polymerization process (Mitra and Sept 2008). Thus, they bind tubulin with straighter conformation (Kumbhar et al. 2019).

In vertebrates' cells, several α and β tubulins isotypes are present, namely tubulins differing in amino acid sequence, with 90% of similarity among them (Massarotti et al. 2012). Isotypes are expressed in different quantities in the various human tissues and they are characterized by different binding affinities for various anti-cancer agents (Kumbhar et al. 2016). Cancer cells overexpress isotypes that are less expressed in healthy tissue (Santoshi and Naik 2014): targeting an isotype mostly expressed by cancer cells increases specificity and decreases systemic effects (Huzil, Mane, and Tuszynski 2010).

In summary, the alteration of the MT dynamic equilibrium can affect the cell cycle and may lead to the arrest of mitosis and cell death. Antimitotic drugs, like Colchicine and Taxol, cause the alteration of dynamic instability, property particularly exploited in anti-cancerous therapies. Several tubulin isotypes are expressed in human tissues, and the same compound binds them with different affinity. Moreover, external stimuli suffered by the cell, such as exposure to anticancer drugs, affect the isotypes expression: this offers an advantage to rationally refine the drug design, by searching for more effective compounds capable of causing fewer systemic effects.
Lately, the use of computational techniques has significantly increased, mainly thanks to the advances made in the field of computer science. More specifically, it is now possible to simulate biological systems made up of a huge number of molecules. Several tools, such as Molecular Dynamics (MD), allow to study biological systems and their physical properties with atomistic resolution.

Computational methods are a powerful instrument for research and investigation of biological processes. In this master thesis, these approaches offer the opportunity to examine in detail, with atomistic resolution, the effects caused by the interaction between drug and tubulin, i.e. both local and global conformational changes induced on the tubulin dimer.

The purpose of this research study is to improve the knowledge on the mechanisms of action of two well known drugs, Colchicine and Taxol. Specifically, this study focuses on the molecular mechanisms that characterize their binding to the two tubulin isotypes most expressed in human tissues.

In detail, Molecular Dynamics simulations where executed on human tubulin isotypes, bound and unbound to the two antimitotic agents. This allows differences and commonalities to be identified between the mechanisms of action of drugs and between the effects induced on different tubulin isotypes.

4.3 Materials and methods

In this work, human tubulin isotypes αβI and αβIVb were used since they are the most widely expressed in all types of human tissue, excluding the brain (Leandro-García et al. 2010). Tubulin isotype IVb has a total of 11 mutations compared to the tubulin isotype I: 7Ile to Leu, 45Asp to Glu, 48Ser to Asn, 64Ile to Val, 293Val to Met, 364Ala to Ser, 365Val to Ala, 434Glu to Gly, 435Asp to Glu, 437Gly to Glu, 444Ala to Val. All these mutations occur outside the Colchicine and Vinca binding site, but very close to the Taxol binding site.

4.3.1 Homology modelling of tubulin isotypes

Human tubulin isotypes αβI and αβIVb, since they haven't been solved yet, were built by means of homology modelling, using 4O2B.pdb and 1JFF.pdb from the RSCB database as template for tubulin dimer bound to Colchicine and Taxol, respectively. The same structures, deprived of the drug, have been used as a comparative element in the evaluation of drug's activity. These structures were chosen since they were solved when bound to the relative drug.

From the starting pdb files only one tubulin dimer (α and β monomers), the GTP, the GDP and Mg^{2+} were extracted. Colchicine's coordinates were obtained from the 4O2B structure, while Taxol's ones from the 1JFF. Missing residues (276-281 in β tubulin of 4O2B and 1, 35-60 in α tubulin and 1 in β of 1JFF) were added using MODELLER 9.22 and the best model was chosen based on the zDOPE (Discrete optimized protein energy) score.

From Uniprot website Fasta sequences of the tubulin isotypes were downloaded: sequence Q71U36 was used for the α chain, sequence P07437 was used for βI chain and sequence P68371 was used for βIVb chain. The α chain sequence is the same for both dimer isotypes because the tubulin mostly involved in drug binding is β tubulin (Huzil, Ludueña, and Tuszynski 2006). Then, homology modelling was performed using the MODELLER 9.22 software.

4.3.2 System set up

Each structure modelled as previously described was studied by molecular dynamics simulations both in presence and in absence of the two investigated drugs. Therefore, eight structures have been carried out.

Software GROMACS 2019.3 was used to perform MD simulations. For the generation of chain topologies, the AMBER ff99SB-ILDN forcefield was chosen, while topologies for GTP, GDP, Colchicine and Taxol were built using ANTECHAMBER module. General amber force field and BCC charge method were used, and ACPYPE tool has been used to convert topologies in GROMACS format. All structures were placed in a

dodecahedron box with minimum distance between solute and box of 0.7 nm and periodic boundary conditions were applied. Next, boxes were solvated using TIP3P explicit water model. System charge was neutralized by adding sodium and chlorine ions, setting an ion concentration of 150 mM. Minimization was executed though means of steepest descent algorithm, with 5000 steps and a maximum force of 100 $kJmol^{-1}nm^{-1}$. Then equilibrations were carried out in NVT and NPT ensemble applying position restrains on the systems, except on water molecules, sodium and chloride ions. The NVT equilibration was executed for 100 ps, with velocity-rescale thermostat with tau constant equal to 0.1 and reference temperature set to 300 K. NPT equilibration was executed for 300 ps, with Berendsen barostat and reference pressure of 1 atm. For electrostatic calculations Particle-mesh Ewald (PME) method has been used, setting cut-off to 1.0 nm, Fourier spacing of 0.2 nm and interpolation order of 4. In the end, a 200 ns simulation was carried out without position restrain, using a 2 fs time step and saving solute coordinates every 2 ps. System's replicas were performed in order to ensure the repeatability of the results.

4.3.3 Structural Analysis

The conformation of the dimer arouses great interest in literature, as it greatly influences the polymerization process of the microtubule (Tripathi et al. 2018). To describe the relative arrangement of the two dimers, the bending angle (θ) and the torsion or twisting angle (ϕ) relating to the straight conformation of the dimer incorporated in the microtubule were calculated. Before proceeding, the principal component analysis (PCA) was performed: trajectories were filtered on the eigenvectors that alone make up 50% of the sum of all eigenvalues. In this way the trajectories were cleaned from minor motions, emphasizing the main ones. The internal beta sheets of α subunit of each structure was then fitted on relative ones belonging to a dimer inside the microtubule. This reference structure was extracted from the structure 3J6F.pdb, which represents a portion of the microtubule wall. Internal sheets in α subunit were: S4 (133-139), S5 (164-171), S6 (199-203), S7 (269-272), S8 (311-319) and S10 (373-380). They were chosen because they are very rigid structures within the monomer, as shown by their low RMSD, always lower than 0.2 nm (Supporting Information, Figure 4.9). With all these expedients, in the obtained trajectories the alpha chain remains still during the simulation, while the beta chain moves relatively to it. The calculated bending and twisting angles are absolute measures with respect to the structure of the dimer inside the microtubule.

To calculate the bending angle (θ), three reference points have been taken into account: the centre of mass (COM) of the internal beta sheets of the α monomer (1), the COM of the internal beta sheets of the β monomer (2) and the COM of both internal beta sheets (3). The definition of these three reference

points allows to define two vectors (A-axis and B-axis). A-axis was defined by points 3 and 1 in the first frame of the simulation. The B-axis (B) is defined by points 2 and 3, with 3 fixed at the first frame position. B-axis orientation varies in each frame of the simulation, while A-axis is fixed. The angle intercepted by these two vectors provides a measure of the bending angle. The twisting angle variation (ϕ) was instead calculated as the angle subtended by the axis of the sheet S10 of β monomer with respect to its starting position. All angle values have been scaled relative to the structure in the wall (3J6F dimer structure).

4.3.4 Derivation of energy landscape

To obtain the energy states associated with each angular value, the Boltzmann Inversion (BI) was performed. First, the angles distribution along the 200 ns of simulation was obtained. Then, the probability of obtaining a certain pair of bending-twisting angle values has been calculated, that is the probability of obtaining a certain conformational state. Once the probability P is obtained, Bolzmann Inversion can be perfomed by applying the following formula:

$$V\ (b,t)\ =\ -\ k_B T\ N_A \ln\ (P\ (b,t))$$

where k_B is the Boltzmann constant, T is the temperature in Kelvin and N_A is the Avogadro number. P (b,t) means that probability is a variable function of bending (b) and twisting angle (t).

4.4 Results and Discussion

First, RMSD analysis was performed on all systems, to make sure that the structures were in equilibrium (Figure 4.1). Moreover, clustering was performed on the last 50 ns, with RMSD cut off 0.15 nm. For each structure only one cluster was obtained, ensuring the equilibrium in the last part of the simulation.

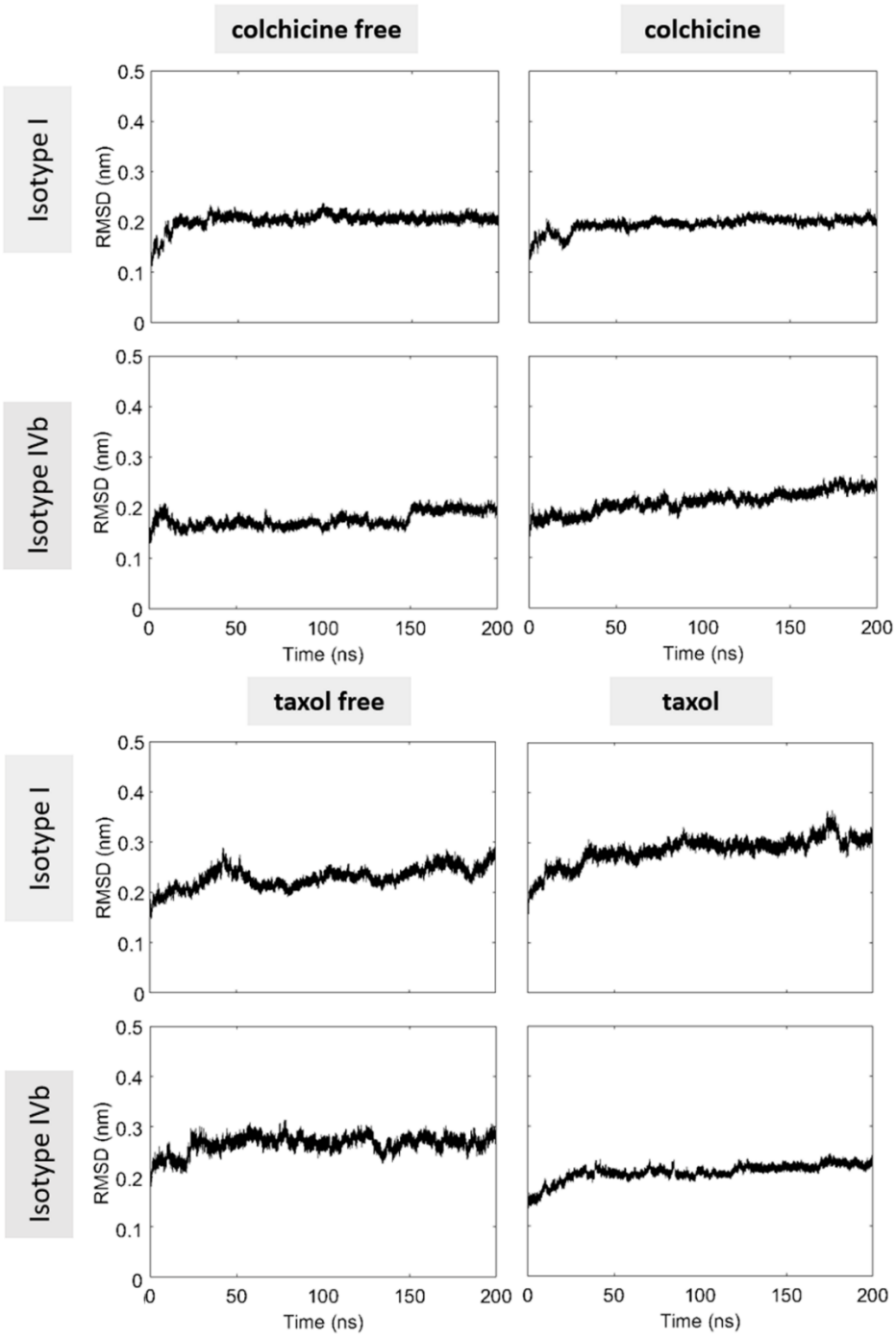

Figure 4.1: RMSD analysis results.

In order to study global effects induced by the presence of ligands in the system, the root mean square fluctuations (RMSF) were analysed. For each substructure, the differences between the highest RMSF value of drug bound and drug free system were calculated. Only structures with significant fluctuations (> 0.05 nm) have been considered (Figure 4.2). Since β chain is the most studied in literature and since both drugs mainly interact with β chain, attention has been focused solely on it.

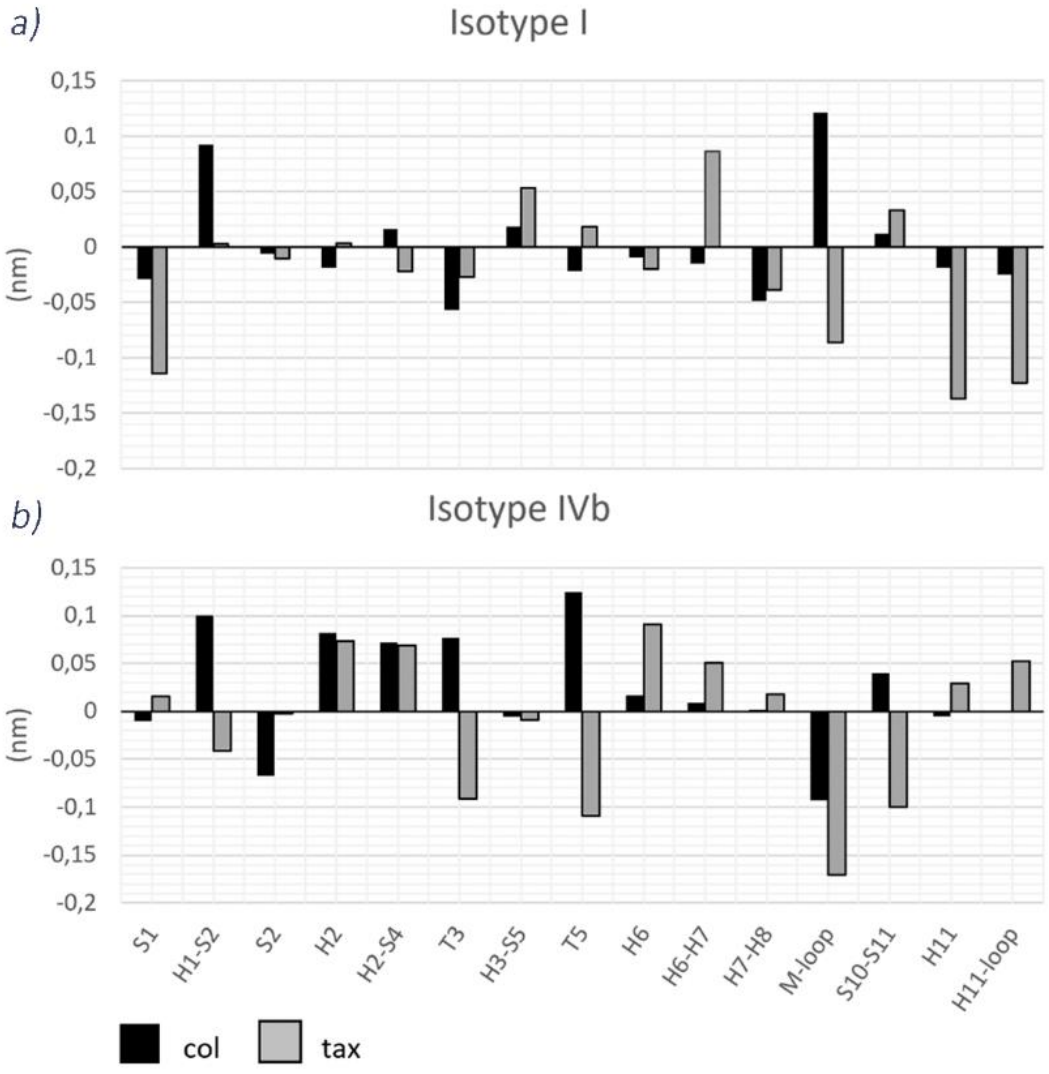

Figure 4.2: RMSF fluctuations for isotype I (a) and isotype IVb (b). For each substructure, the differences between the highest value of drug bound (Colchicine in black, Taxol in gray) and drug free systems are plotted. Only significant differences (> 0.05 nm) are maintained.

Both drugs in general have different effects on the two isotypes, except for the substructures H1-S2 loop for Colchicine and M-loop for Taxol: Colchicine always increases H1-S2 loop fluctuations, in both isotypes, while Taxol always decreases M loop fluctuations. The H1-S2 loop interacts with the M-loop in the lateral interactions within the protofilaments in the microtubule (Löwe et al. 2001). It is worth mentioning that no structures belonging to the Colchicine binding site are shown in Figure 4.2: this means that Colchicine mostly interacts without changing local fluctuations, inducing variations only outside its binding site.

Moreover, in order to study the local effects induced by the presence of the drugs, the secondary structure of binding sites has been analysed. Colchicine binding site is constituted by S8 (310-317) and S9 (347-353) sheets, H7 (221-239) and H8 (249-256) helices and T7 loop (240-248) of β tubulin, and by T5 (172-180) loop of α chain (Tripathi et al. 2018). The secondary structure analysis was carried out using STRIDE (Heinig and Frishman 2004) during the last 50 ns of simulation. The probabilities of secondary structure were obtained for each residue, so they have been averaged in order to obtain the probability for each substructure constituting the Colchicine binding site, as reported in Figure 4.3.

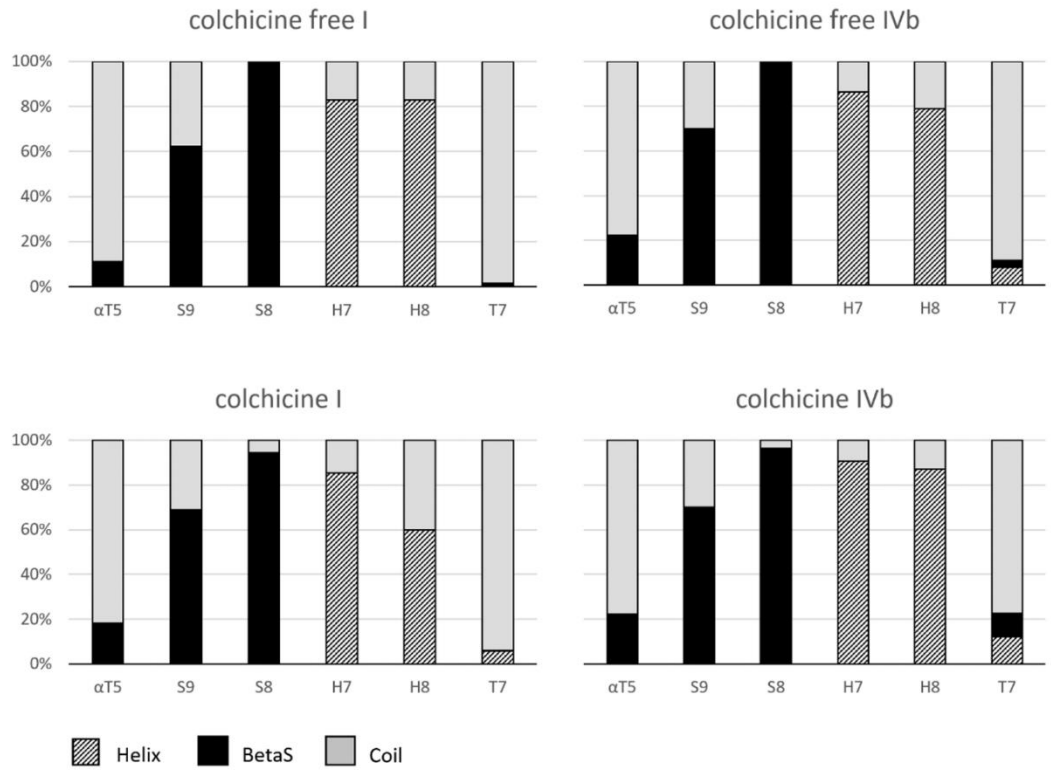

Figure 4.3: probability of secondary structure of Colchicine binding site. Helix is illustrated with a stripe pattern, beta sheet is represented in black and coil in grey.

As shown in Figure 4.3, the secondary structure does not substantially change for both isotypes when the Colchicine binds: this is in accordance with RMSF data, showing that Colchicine does not induce significant variations in its binding site. Only T7 loop showed to be slightly more structured in the presence of Colchicine: this could be in accordance with what stated in recent literature (Dorléans et al. 2009; Pascale Barbier et al. 2010; Prota et al. 2014), claiming that the structural differences particularly involve the T7 loop.

The Taxol binding site is only located in β tubulin, and it is made up of H7 (221-239) helix, S7 (265-270) sheet, H6-H7 (215-221) and S9-S10 (354-362) loops and M loop (271-284) (Prota et al. 2013). The structure of the Taxol binding site was analysed using the same technique described for Colchicine (Figure 4.4).

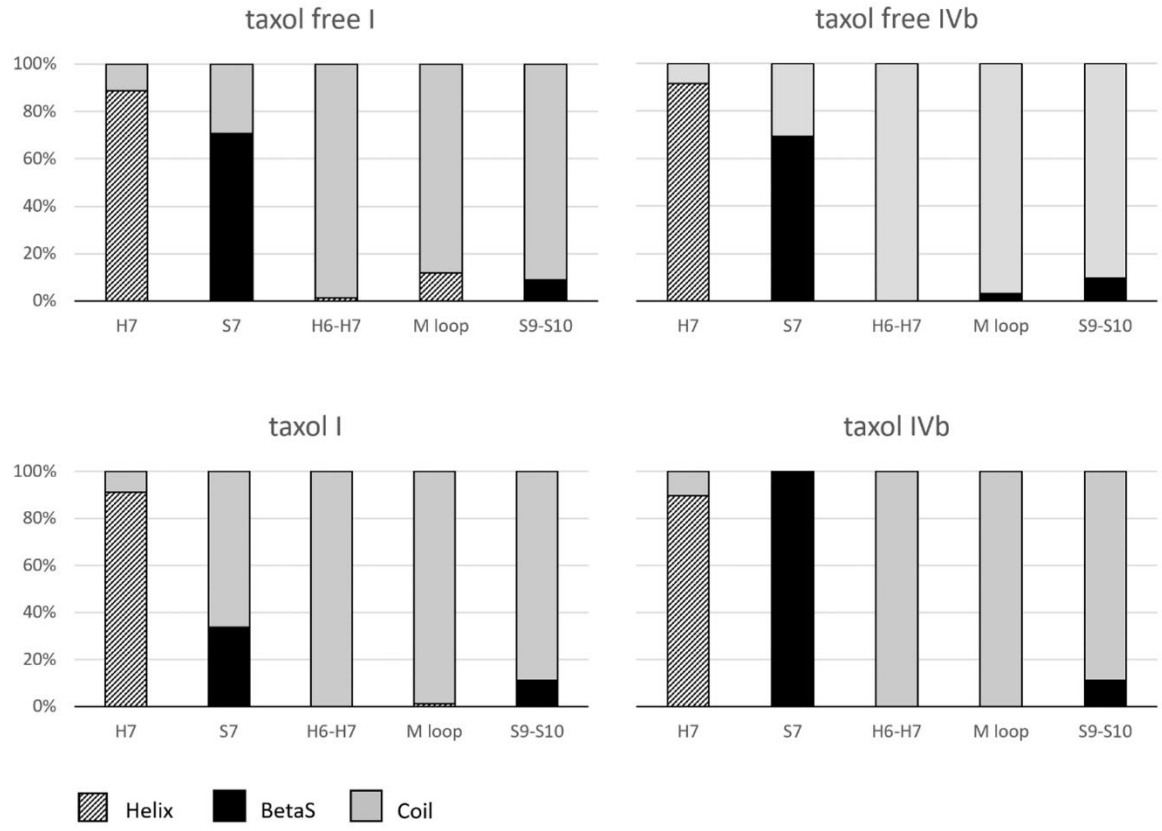

Figure 4.4: probability of secondary structure of Taxol binding site. Helix is illustrated with a stripe pattern, beta sheet is represented in black and coil in grey.

Taxol affects the structure of S7 sheet, decreasing in isotype I, and raising in isotype IVb with respect to the ligand free protein. However, this substructure is not directly associated with the dimer-dimer

interactions within the microtubule and therefore its modification is not supposed to efficiently alter the microtubule dynamics. The different behaviour between the two isotypes is very interesting, because it may be due to mutations of the isotype IVb compared to the isotype I: these mutations are 364Ala to Ser and 365Val to Ala, close to the Taxol binding site, near the S9-S10 loop, which could change the Taxol mode of interaction with the sheet. Since the H1-S2 loop and the M loop are both involved in the lateral interactions between the dimers, their secondary structures have been more in depth analysed (Figure 4.5).

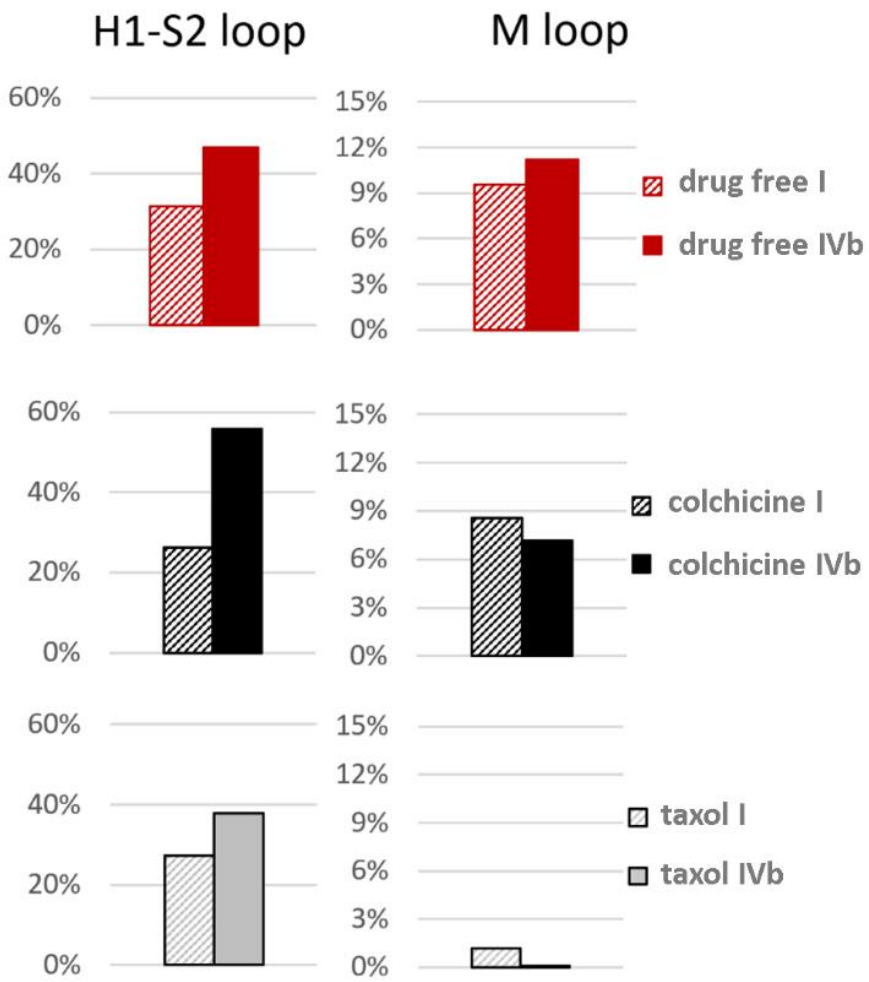

Figure 4.5: percentage of secondary structure of H1-S2 loop and M loop. Isotype 1 is represented with stripe pattern, isotype 4b is reported withuout pattern. Structure without drug is shown in red, systems bound with Colchicine is black painted, system bound to Taxol is grey painted.

About the H1-S2 loop, both drugs have a moderate effect in the isotype I, while in isotype IVb Colchicine raise the percentage of secondary structure and Taxol decreases it. About the M loop, there is a clear contrast between Colchicine and Taxol in both isotypes. Colchicine maintains the secondary structure of the M loop in isotype I and slightly decreases it in isotype IVb, while Taxol destabilizes it almost totally in isotype I, and totally in isotype IVb. The different effects induced by Colchicine and Taxol could be related to the fact that they are two different types of drug: Colchicine is a destabilizing drug, while Taxol is a stabilizer, so it is interesting that the effects on the M loop, involved in interactions with adjacent dimers, are opposites.

The dimer conformational changes were also analysed. To do this, the trajectories fitted on the internal beta sheets of the alpha subunit were used. The Principal Component Analysis (PCA) was carried out, in order to filter the trajectories on the eigenvectors which alone constitute the 50% of the sum of all eigenvalues. In this way it is possible to remove the minor motions, highlighting the main ones, on which the analyses are carried out. Results are shown in Figure 4.6.

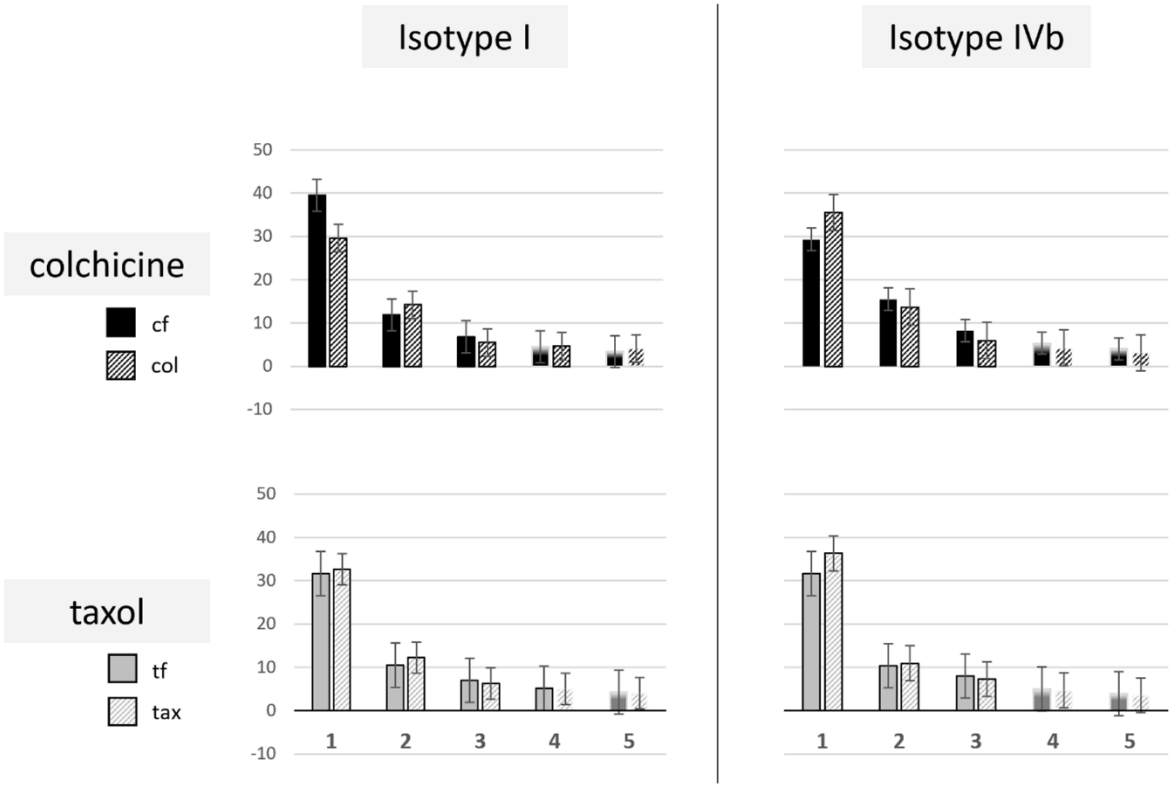

Figure 4.6: percentage contribution of the first five eigenvectors obtained by PCA analysis. Eigenvectors represented with shading edges exceed 50% of the total contribution.

Only first five eigenvectors are shown, as they are the most energetic ones. Colchicine decreases the percentage contribution of the first eigenvalue in isotype I, while the reverse effect is induced in isotype IVb, although with lesser evidence. Taxol, on the other hand, does not produce significant changes in the percentage contributions of the first eigenvectors. This means that the Colchicine modifies more the most important motions of the dimer, and in the opposite way between the two isotypes, while the Taxol has a lesser influence.

Given the importance of the tubulin dimer conformational behaviour in microtubule dynamics, the energy states associated with bending and twisting angles were calculated. To obtain the energy states associated with each angular value, the Boltzmann Inversion (BI) was performed. The energy landscapes constitute a three-dimensional surface, whose depth depends on the angular coordinates.

Data represented in Figure 4.7 were obtained by combining the trajectories of both studied isotypes, to directly evaluate the general effects of the drug on the isotypes most expressed in human tissues: together, isotype I and isotype IVb account for 45% to more than 95% of the tubulin isotypes expressed by human tissues, with the exception of the brain (Leandro-García et al. 2010).

In Figure 4.7, the first column on the left shows the energy values associated with the pairs of twisting - bending angles values, with the twisting angles on the abscissae axis, and the bending angles on the ordinate axis. A colormap defines the energy value associated with the coordinates. Every single point in the twisting-bending angle graph corresponds to a conformational state of the state space. The smaller the white area within the graph, the greater the exploration of state space. The darker the area represented within the graph, the greater the energy associated with that state, and therefore the greater the probability of finding the relative angular values in the structure under examination. The second and third columns are the projection of the energy surface on the bending-energy plane and twisting-energy plane, respectively.

Colchicine and Taxol affect tubulin internal bending in a different way.

Colchicine stiffens bending, while Taxol makes tubulin less rigid to bending with respect to the ligand free protein. This can be seen by analysing the range of the bending angles explored by the two systems: it is decreased in the presence of the Colchicine, while it is increased in the presence of the Taxol.

In addition, Colchicine has a very low peak at a bending angle of 10 degrees: once this configuration is reached, it is much more difficult for the Colchicine-bound structure to move away from it, because of the depth of the peak: the energy state associated to this configuration is very favourable, therefore the

system will evolve in the space of the states tending more to reach the state associated to the peak. Both drugs affect twisting in the same way, and it is stiffened in both cases: in fact, the range of the explored angles decreases in the presence of both Taxol and Colchicine and is the same between the two drugs.

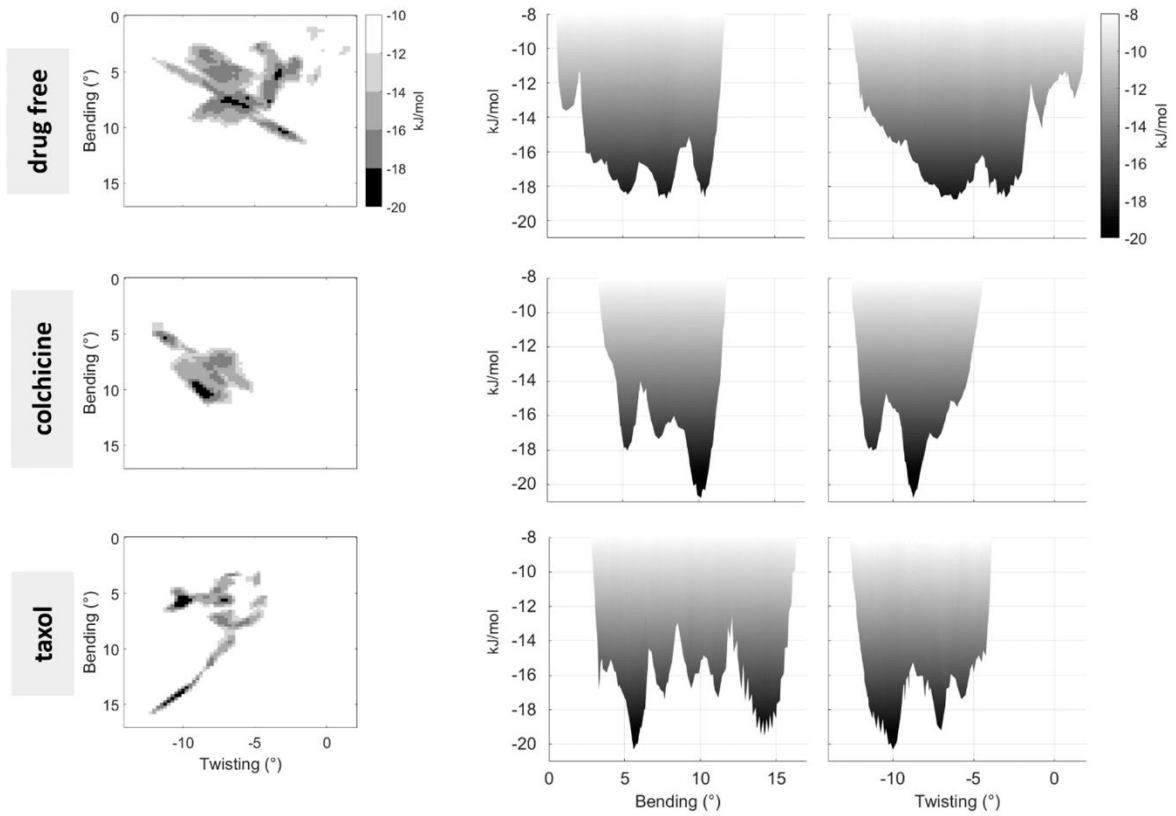

Figure 4.7: energy landscape as a function of angular values.

The results obtained suggest that Colchicine can counteract the bending movement: the stiffening of this movement contrasts the integration of the dimer in the microtubule lattice, resulting in a destabilizing effect (Dorléans et al. 2009). The opposite behaviour is obtained with Taxol, which instead decreases the bending stiffness. A lower stiffness could allow the dimer to more easily adapt to the microtubule lattice and to any possible movements of the microtubule itself, thus stabilizing it (Pampaloni and Florin 2008).

It is worth of interest that Colchicine affects bending and twisting in a similar way in both isotypes (Supporting information, Figure 4.10).

Concerning Taxol, it influences twisting angle in a similar way in both isotypes (Supporting information, Figure 4.11), while a different effect was exhibited in the bending motion (Figure 4.8).

As it can be seen from Figure 4.8, in isotype I the bending motion is strongly limited by the presence of Taxol, while in isotype IVb Taxol tubulin increases the range of explored bending angles. This difference could be ascribed to mutations typical of isotype IVb compared to isotype I, which are located close to the Taxol binding site (S9-S10 loop). Specific isotype mutations can highly influence binding effects induced by the presence of the drug, since those mutations modify the physical-chemical characteristics of the tubulin binding cleft and hence the way the drug is bound in its tubulin site.

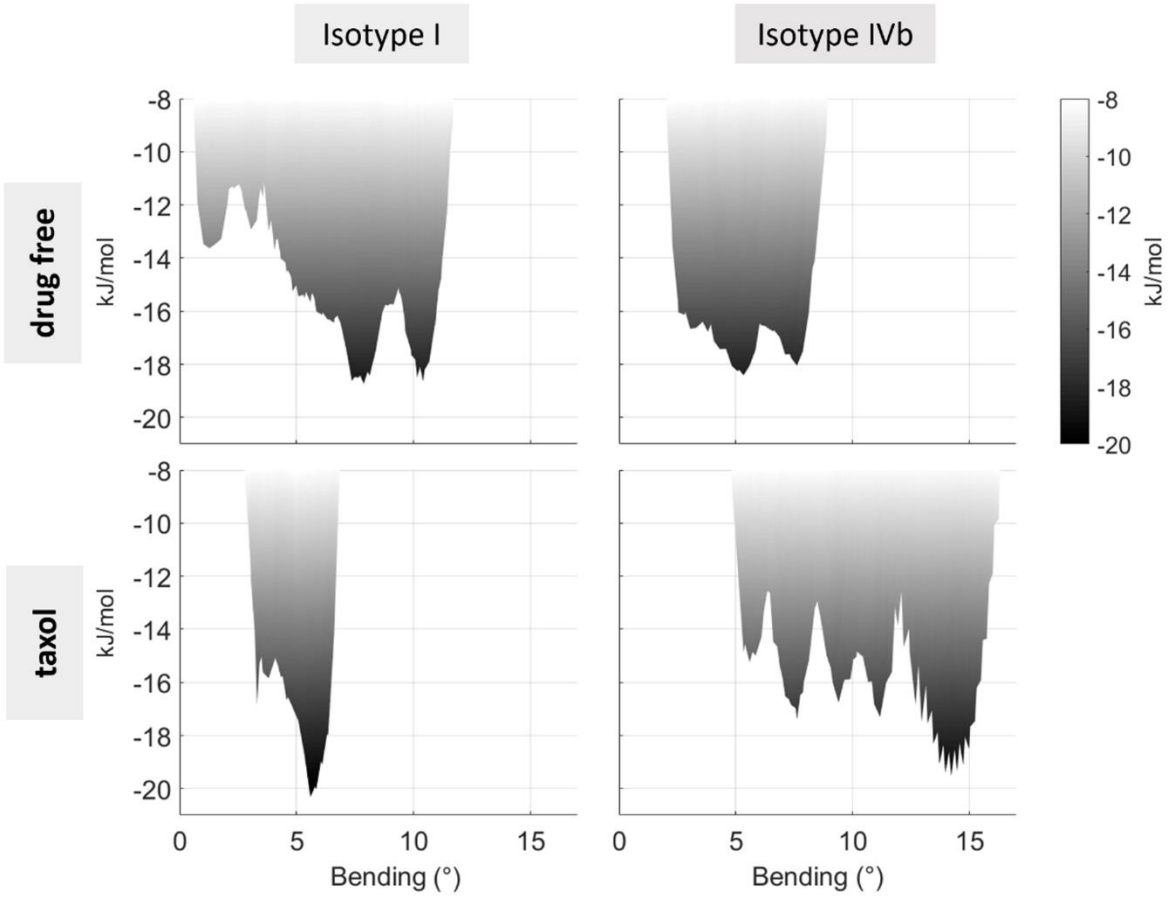

Figure 4.8: bending energy landscapes of drug free system and Taxol bound system.

4.5 Conclusions

Overall, the mechanism of action characterizing Colchicine and Taxol binding can be completely different, and in several specific characteristics they act in an opposite way on the tubulin structural features.

By comparing the data of driven tubulin secondary structures and RMSF residue fluctuations, it is possible to hypothesize a different mechanism of action exerted on structures involved in lateral contacts: Taxol totally (in isotype IVb) or almost totally (in isotype I) decreases the probability of secondary structure of M loop and stabilizes its fluctuations in both isotypes.

Taxol presence affects M loop driving it to more open and unstructured shaped favouring the possibility to establish stable lateral bonds with an adjacent dimer: a completely unstructured M loop can more easily adapt to a second interacting structure.

Colchicine, on the other hand, affects more the conformation of H1-S2 loop, which showed higher structural order and higher fluctuations in presence of the drug, reducing the probability of lateral interactions.

Therefore, Taxol seems to favour lateral interactions, important for the integration of the dimer inside the microtubule, whereas Colchicine shows an opposite behaviour.

Moreover, considering the energy profiles associated with the angular distributions, Colchicine limits the bending movement, stiffening and forcing it to assume a certain value, equal to 10 degrees. This modification is in line with the idea that Colchicine is a destabilizing drug. A tubulin dimer, when inserted inside the microtubule, is subjected to stresses due to the interaction with other dimers: a more flexible dimer is able to more easily adapt to the new condition, modifying its conformation so as to reduce stresses, while a more rigid dimer is less inclined to adapt its conformation, causing a destabilizing effect on the microtubule. In this context, the effect introduced by Taxol is opposite to that of Colchicine: it increases the possibility of bending movement, widening the range of exploration and making bending less rigid, therefore with a consequent stabilizing effect.

Further studies are essential to deeper understand action mechanisms of the two drugs. In this context, it would be of great interest to extend the present method of investigation to all the other tubulin isotypes, highlighting any differences or common points.

Moreover, in the field of rational drug design, it will be of primary importance to find a strong correlation between drug affinity and the dimer conformational changes which quantify drug activity. Equally

interesting would be to analyse the behaviour of the dimer within the microtubule lattice: lateral and longitudinal interactions of the adjacent dimers could highlight the effects induced by the presence of the drug, especially on structures such as the H1-S2 loop and the M loop. In this way it would be possible to verify several hypotheses proposed in this work.

4.6 Supporting information

4.6.1 RMSD of internal beta sheets

RMSD of internal beta sheets of alpha subunits are reported. Their low values prove their high stability (Figure 4.9).

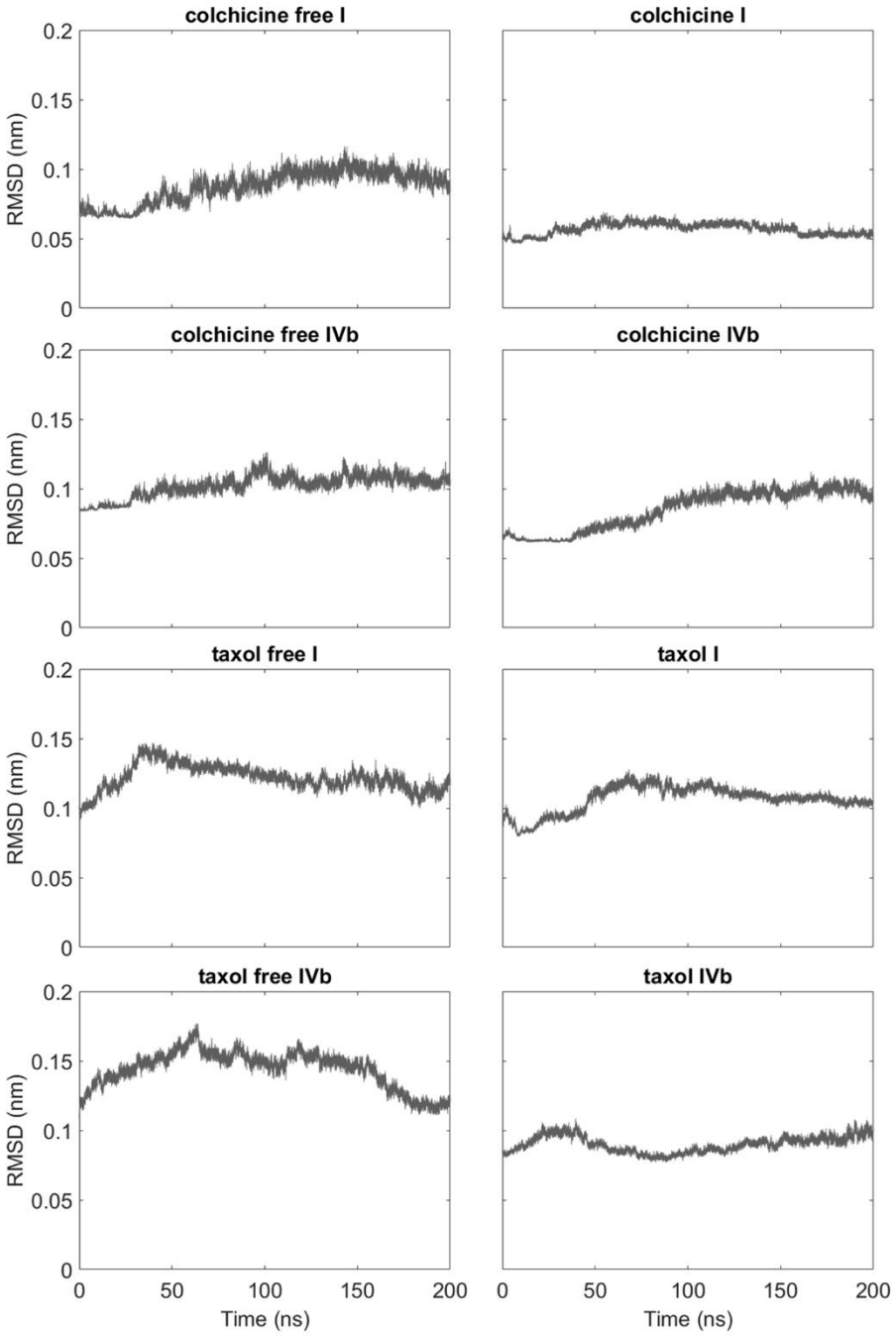

Figure 4.9: RMSD of internal beta sheets of alpha subunit.

4.6.2 Energy landscapes as a function of angular values

Energy landscapes for bending and twisting angles have been calculated, for both isotypes and for drug free and drug bound systems. Results are shown in Figure 4.10 and Figure 4.11.

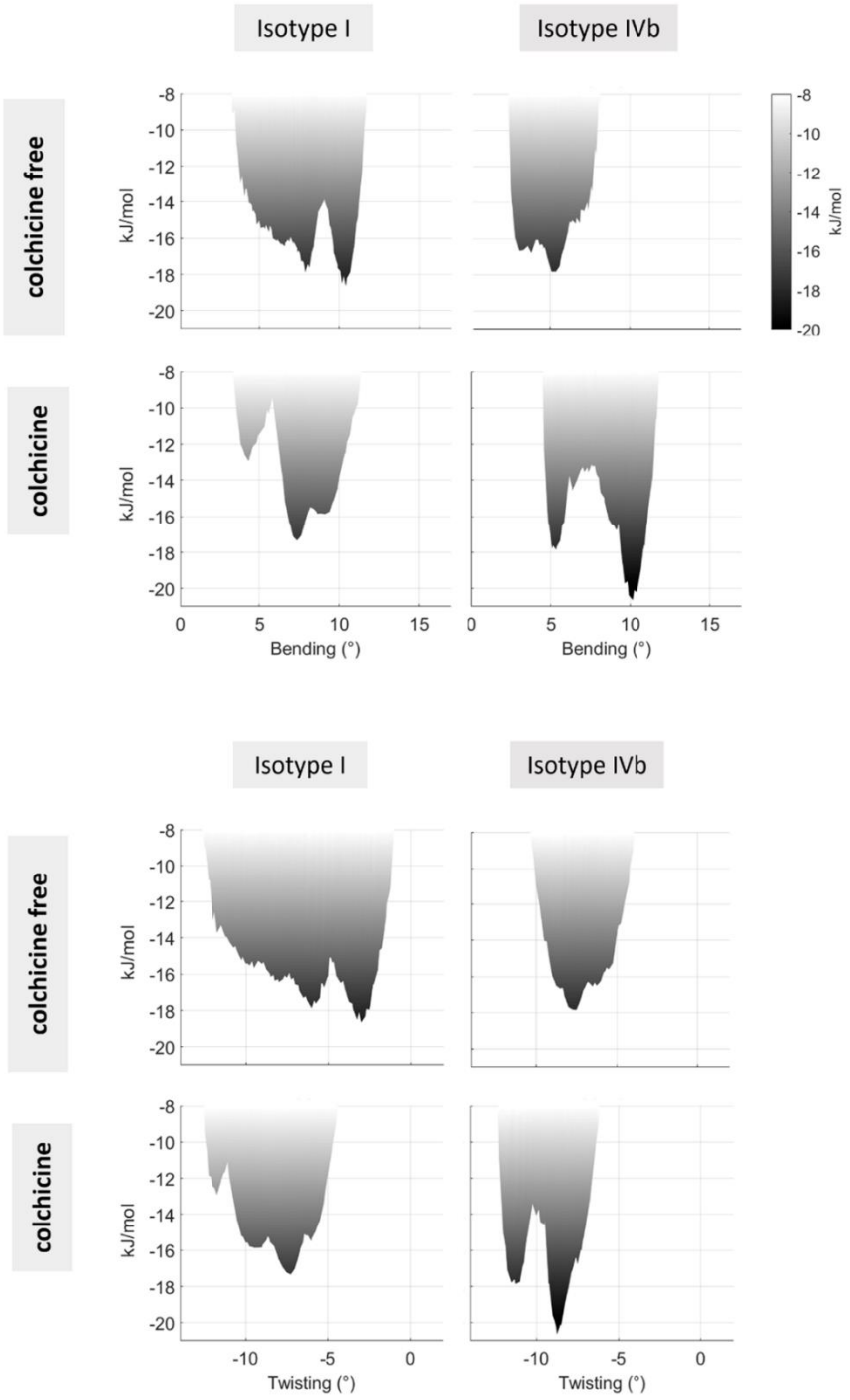

Figure 4.10: energy landscapes for bending and twisting angles of Colchicine free and Colchicine bound systems.

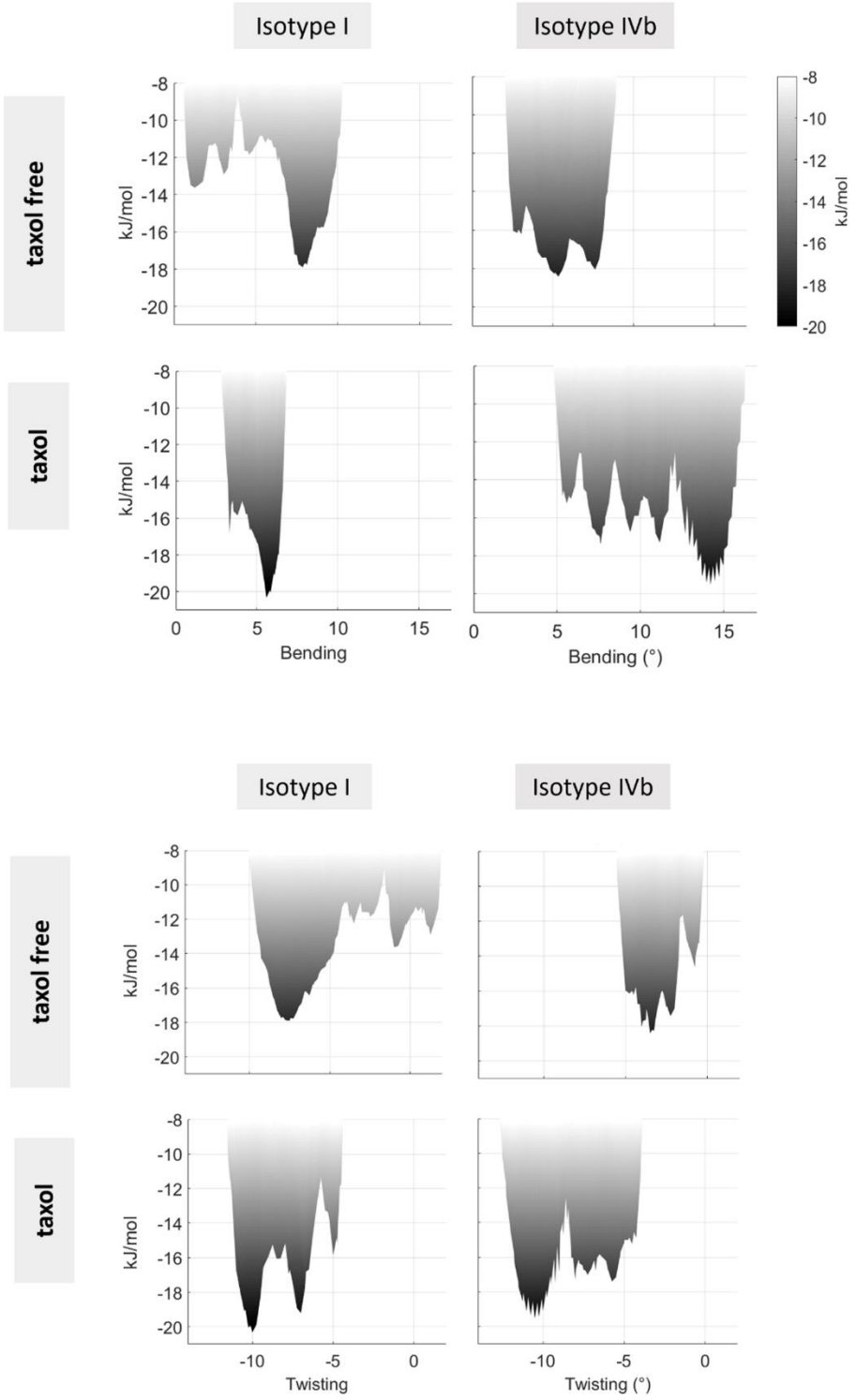

Figure 4.11: energy landscapes for bending and twisting angles of Taxol free and Taxol bound systems.

5 References

- Abraham, Mark James, Teemu Murtola, Roland Schulz, Szilárd Páll, Jeremy C. Smith, Berk Hess, and Erik Lindahl. 2015. "GROMACS: High Performance Molecular Simulations through Multi-Level Parallelism from Laptops to Supercomputers." *SoftwareX* 1–2 (September): 19–25. https://doi.org/10.1016/j.softx.2015.06.001.

- Barbier, P., P. O. Tsvetkov, G. Breuzard, and F. Devred. 2014. "Deciphering the Molecular Mechanisms of Anti-Tubulin Plant Derived Drugs." *Phytochemistry Reviews* 13 (1): 157–69. https://doi.org/10.1007/s11101-013-9302-8.

- Barbier, Pascale, Audrey Dorléans, Francois Devred, Laura Sanz, Diane Allegro, Carlos Alfonso, Marcel Knossow, Vincent Peyrot, and Jose M. Andreu. 2010. "Stathmin and Interfacial Microtubule Inhibitors Recognize a Naturally Curved Conformation of Tubulin Dimers." *Journal of Biological Chemistry* 285 (41): 31672–81. https://doi.org/10.1074/jbc.M110.141929.

- Bennett, M J, J K Chik, G W Slysz, T Luchko, J Tuszynski, D L Sackett, and D C Schriemer. 2009. "Structural Mass Spectrometry of the Aβ-Tubulin Dimer Supports a Revised Model of Microtubule Assembly." *Biochemistry* 48 (22): 4858–70. https://doi.org/10.1021/bi900200q.

- Botta, Maurizio, Stefano Forli, Matteo Magnani, and Fabrizio Manetti. 2009. "Molecular Modeling Approaches to Study the Binding Mode on Tubulin of Microtubule Destabilizing and Stabilizing Agents." *Topics in Current Chemistry* 286: 279–328. https://doi.org/10.1007/128_2008_20.

- Case, David A., Thomas E. Cheatham, Tom Darden, Holger Gohlke, Ray Luo, Kenneth M. Merz, Alexey Onufriev, Carlos Simmerling, Bing Wang, and Robert J. Woods. 2005. "The Amber Biomolecular Simulation Programs." *Journal of Computational Chemistry* 26 (16): 1668–88. https://doi.org/10.1002/jcc.20290.

- Coderch, Claire, Antonio Morreale, and Federico Gago. 2012. "Tubulin-Based Structure-Affinity Relationships for Antimitotic Vinca Alkaloids." *Anti-Cancer Agents in Medicinal Chemistry* 12 (3): 219–25. https://doi.org/10.2174/187152012800228841.

- Darden, Tom, Darrin York, and Lee Pedersen. 1993. “Particle Mesh Ewald: An N·log(N) Method for Ewald Sums in Large Systems.” *The Journal of Chemical Physics* 98 (12): 10089. https://doi.org/10.1063/1.464397.

- Deriu, Marco Agostino, Monica Soncini, Mario Orsi, Mishal Patel, Jonathan W Essex, Franco Maria Montevecchi, and Alberto Redaelli. 2010. “Anisotropic Elastic Network Modeling of Entire Microtubules.” *Biophysical Journal* 99 (7): 2190–99. https://doi.org/10.1016/j.bpj.2010.06.070.

- Desai, A, and T J Mitchison. 1997. “Microtubule Polymerization Dynamics.” *Annual Review of Cell and Developmental Biology* 13 (January): 83–117. https://doi.org/10.1146/annurev.cellbio.13.1.83.

- Devred, Francois, Philipp O Tsvetkov, Pascale Barbier, Diane Allegro, Susan Band Horwitz, Alexander A Makarov, and Vincent Peyrot. 2008. “Stathmin/Op18 Is a Novel Mediator of Vinblastine Activity.” *FEBS Letters* 582 (17): 2484–88. https://doi.org/10.1016/j.febslet.2008.06.035.

- Dorléans, Audrey, Benoît Gigant, Raimond B.G. Ravelli, Patrick Mailliet, Vincent Mikol, and Marcel Knossow. 2009. “Variations in the Colchicine-Binding Domain Provide Insight into the Structural Switch of Tubulin.” *Proceedings of the National Academy of Sciences of the United States of America* 106 (33): 13775–79. https://doi.org/10.1073/pnas.0904223106.

- Grafmüller, Andrea, and Gregory A. Voth. 2011. “Intrinsic Bending of Microtubule Protofilaments.” *Structure* 19 (3): 409–17. https://doi.org/10.1016/j.str.2010.12.020.

- Heinig, Matthias, and Dmitrij Frishman. 2004. “STRIDE: A Web Server for Secondary Structure Assignment from Known Atomic Coordinates of Proteins.” *Nucleic Acids Research* 32 (Web Server issue): W500–502. https://doi.org/10.1093/nar/gkh429.

- Herman J. C. Berendsen. 2007. *Simulating the Physical World*. *Annals of Physics*. https://doi.org/10.1017/CBO9780511815348.

- Hess, Berk, Carsten Kutzner, David van der Spoel, and Erik Lindahl. 2008. “GROMACS 4: Algorithms for Highly Efficient, Load-Balanced, and Scalable Molecular Simulation.”

Journal of Chemical Theory and Computation 4 (3): 435–47. https://doi.org/10.1021/ct700301q.

- Huzil, J. Torin, Jonathan Mane, and Jack A. Tuszynski. 2010. "Computer Assisted Design of Second-Generation Colchicine Derivatives." *Interdisciplinary Sciences: Computational Life Sciences* 2 (2): 169–74. https://doi.org/10.1007/s12539-010-0076-z.

- Huzil, J Torin, Ke Chen, Lukasz Kurgan, and Jack A Tuszynski. 2007. "The Roles of Beta-Tubulin Mutations and Isotype Expression in Acquired Drug Resistance." *Cancer Informatics* 3 (April): 159–81.

- Huzil, J Torin, Richard F Ludueña, and Jack Tuszynski. 2006. "Comparative Modelling of Human β Tubulin Isotypes and Implications for Drug Binding." *Nanotechnology* 17 (4): S90–100. https://doi.org/10.1088/0957-4484/17/4/014.

- Igaev, Maxim, and Helmut Grubmüller. 2018. "Microtubule Assembly Governed by Tubulin Allosteric Gain in Flexibility and Lattice Induced Fit." *ELife* 7 (April). https://doi.org/10.7554/eLife.34353.

- Kumbhar, Bajarang Vasant, Vishwambhar Vishnu Bhandare, Dulal Panda, and Ambarish Kunwar. 2019. "Delineating the Interaction of Combretastatin A-4 with Aβ Tubulin Isotypes Present in Drug Resistant Human Lung Carcinoma Using a Molecular Modeling Approach." *Journal of Biomolecular Structure and Dynamics* 0 (0): 1–13. https://doi.org/10.1080/07391102.2019.1577174.

- Kumbhar, Bajarang Vasant, Anubhaw Borogaon, Dulal Panda, and Ambarish Kunwar. 2016. "Exploring the Origin of Differential Binding Affinities of Human Tubulin Isotypes AβII, AβIII and AβIV for DAMA-Colchicine Using Homology Modelling, Molecular Docking and Molecular Dynamics Simulations." Edited by Takashi Toda. *PLOS ONE* 11 (5): e0156048. https://doi.org/10.1371/journal.pone.0156048.

- Leach, Andrew R. 2001. *Molecular Modelling: Principles and Applications*. *Computers*. Vol. 21. Prentice Hall. https://doi.org/10.1016/S0097-8485(96)00029-0.

- Leandro-García, Luis J., Susanna Leskelä, Iñigo Landa, Cristina Montero-Conde, Elena López-

Jiménez, Rocío Letón, Alberto Cascón, Mercedes Robledo, and Cristina Rodríguez-Antona. 2010. “Tumoral and Tissue-Specific Expression of the Major Human β-Tubulin Isotypes.” *Cytoskeleton* 67 (4): 214–23. https://doi.org/10.1002/cm.20436.

- Lee, Hark, and Wei Cai. 2009. “Ewald Summation for Coulomb Interactions in a Periodic Supercell.” *Lecture Notes, Stanford University* 3 (1): 1–12.

- Lee, Hsing, Lee G. Pedersen, Ulrich Essmann, Tom Darden, Lalith Perera, and Max L. Berkowitz. 2002. “A Smooth Particle Mesh Ewald Method.” *The Journal of Chemical Physics* 103 (19): 8577–93. https://doi.org/10.1063/1.470117.

- Löwe, J., H. Li, K. H. Downing, and E. Nogales. 2001. “Refined Structure of Aβ-Tubulin at 3.5 Å Resolution.” *Journal of Molecular Biology* 313 (5): 1045–57. https://doi.org/10.1006/jmbi.2001.5077.

- Mandelkow, E. M., E. Mandelkow, and R. A. Milligan. 1991. “Microtubule Dynamics and Microtubule Caps: A Time-Resolved Cryo-Electron Microscopy Study.” *Journal of Cell Biology* 114 (5): 977–91. https://doi.org/10.1083/jcb.114.5.977.

- Massarotti, Alberto, Antonio Coluccia, Romano Silvestri, Giovanni Sorba, and Andrea Brancale. 2012. “The Tubulin Colchicine Domain: A Molecular Modeling Perspective.” *ChemMedChem* 7 (1): 33–42. https://doi.org/10.1002/cmdc.201100361.

- Mitchison, Tim, and Marc Kirschner. 1984. “Dynamic Instability of Microtubule Growth.” *Nature* 312 (5991): 237–42. https://doi.org/10.1038/312237a0.

- Mitra, Arpita, and David Sept. 2008. “Taxol Allosterically Alters the Dynamics of the Tubulin Dimer and Increases the Flexibility of Microtubules.” *Biophysical Journal* 95 (7): 3252–58. https://doi.org/10.1529/biophysj.108.133884.

- Pampaloni, Francesco, and Ernst-Ludwig Florin. 2008. “Microtubule Architecture: Inspiration for Novel Carbon Nanotube-Based Biomimetic Materials.” *Trends in Biotechnology* 26 (6): 302–10. https://doi.org/10.1016/j.tibtech.2008.03.002.

- Pearlman, D A, D A Case, J W Caldwell, W S Ross, T E Cheatham, S Debolt, D Ferguson, G

Seibel, and P Kollman. 1995. “AMBER, A PACKAGE OF COMPUTER-PROGRAMS FOR APPLYING MOLECULAR MECHANICS, NORMAL-MODE ANALYSIS, MOLECULAR-DYNAMICS AND FREE-ENERGY CALCULATIONS TO SIMULATE THE STRUCTURAL AND ENERGETIC PROPERTIES OF MOLECULES.” *Computer Physics Communications* 91 (1–3): 1–41. https://doi.org/10.1016/0010-4655(95)00041-d.

- Pepe, Antonella, Liang Sun, Ilaria Zanardi, Xinyuan Wu, Cristiano Ferlini, Gabriele Fontana, Ezio Bombardelli, and Iwao Ojima. 2009. “Novel C-Seco-Taxoids Possessing High Potency against Paclitaxel-Resistant Cancer Cell Lines Overexpressing Class III β-Tubulin.” *Bioorganic and Medicinal Chemistry Letters* 19 (12): 3300–3304. https://doi.org/10.1016/j.bmcl.2009.04.070.

- Prota, Andrea E., Franck Danel, Felix Bachmann, Katja Bargsten, Rubén M. Buey, Jens Pohlmann, Stefan Reinelt, Heidi Lane, and Michel O. Steinmetz. 2014. “The Novel Microtubule-Destabilizing Drug BAL27862 Binds to the Colchicine Site of Tubulin with Distinct Effects on Microtubule Organization.” *Journal of Molecular Biology* 426 (8): 1848–60. https://doi.org/10.1016/j.jmb.2014.02.005.

- Prota, Andrea E, Katja Bargsten, Didier Zurwerra, Jessica J Field, José Fernando Díaz, Karl-Heinz Altmann, and Michel O Steinmetz. 2013. “Molecular Mechanism of Action of Microtubule-Stabilizing Anticancer Agents.” *Science* 339 (6119): 587. https://doi.org/10.1126/science.1230582.

- Rendine, Stefano, Stefano Pieraccini, and Maurizio Sironi. 2010. “Vinblastine Perturbation of Tubulin Protofilament Structure: A Computational Insight.” *Physical Chemistry Chemical Physics* 12 (47): 15530–36. https://doi.org/10.1039/c0cp00594k.

- Santoshi, Seneha, and Pradeep K. Naik. 2014. “Molecular Insight of Isotypes Specific β-Tubulin Interaction of Tubulin Heterodimer with Noscapinoids.” *Journal of Computer-Aided Molecular Design* 28 (7): 751–63. https://doi.org/10.1007/s10822-014-9756-9.

- Spoel, David Van Der, Erik Lindahl, Berk Hess, Gerrit Groenhof, Alan E Mark, and Herman J. C. Berendsen. 2005. “GROMACS: Fast, Flexible, and Free.” *Journal of Computational Chemistry* 26 (16): 1701–18. https://doi.org/10.1002/jcc.20291.

- Sprenger, K. G., Vance W. Jaeger, and Jim Pfaendtner. 2015. “The General AMBER Force Field (GAFF) Can Accurately Predict Thermodynamic and Transport Properties of Many Ionic Liquids.” *Journal of Physical Chemistry B* 119 (18): 5882–95. https://doi.org/10.1021/acs.jpcb.5b00689.

- Stanton, Richard A., Kim M. Gernert, James H. Nettles, and Ritu Aneja. 2011. “Drugs That Target Dynamic Microtubules: A New Molecular Perspective.” *Medicinal Research Reviews* 31 (3): 443–81. https://doi.org/10.1002/med.20242.

- Tripathi, Shubhandra, Gaurava Srivastava, Aastha Singh, A. P. Prakasham, Arvind S. Negi, and Ashok Sharma. 2018. “Insight into Microtubule Destabilization Mechanism of 3,4,5-Trimethoxyphenyl Indanone Derivatives Using Molecular Dynamics Simulation and Conformational Modes Analysis.” *Journal of Computer-Aided Molecular Design* 32 (4): 559–72. https://doi.org/10.1007/s10822-018-0109-y.

- VanBuren, Vincent, David J Odde, and Lynne Cassimeris. 2002. “Estimates of Lateral and Longitudinal Bond Energies within the Microtubule Lattice.” *Proceedings of the National Academy of Sciences of the United States of America* 99 (9): 6035–40. https://doi.org/10.1073/pnas.092504999.

- Vertessy, Beata G, Veronika Harmat, Zsolt Böcskei, Gábor Náray-Szabó, Ferenc Orosz, and Judit Ovádi. 1998. “Simultaneous Binding of Drugs with Different Chemical Structures to Ca2+-Calmodulin: Crystallographic and Spectroscopic Studies,.” *Biochemistry* 37 (44): 15300–310. https://doi.org/10.1021/bi980795a.